ACTA MEDICA (HRADEC KRÁLOVÉ)

2016, Vol. 59, No. 4

CONTENTS

ORIGINAL ARTICLES

CASE REPORTS

ORIGINAL ARTICLE

Histological Evaluation of Decellularized Skeletal Muscle Tissue Using Two Different Decellularization Agents

Hana Hrebíková, Magda Voborníková, Milada Hetešová, Jaroslav Mokrý*

Department of Histology and Embryology, Charles University, Medical Faculty, Hradec Králové, Czech Republic
* Corresponding author: Department of Histology and Embryology, Charles University, Medical Faculty, Šimkova 870, 500 03 Hradec Králové, Czech Republic; e-mail: hrebikh@lfhk.cuni.cz

Summary: The aim of the present study was to determine effect of two decellularized agents, sodium dodecyl sulphate (SDS) and Triton X-100, to the skeletal muscle tissue. Final scaffold was evaluated by several histological techniques to analyse preservation of essential structures including collagen and elastic fibres, basement membranes, glycosaminoglycans and also to confirm elimination of nuclear and cytoplasmic components which are redundant in effectively prepared decellularized scaffolds. Comparison of tissue scaffolds processed with different detergents proved that SDS is superior to Triton X-100 as it can effectively decellularize muscle tissue.

Keywords: *Decellularized scaffold; Histology; Skeletal muscle; SDS; Triton X-100*

Introduction

A tissue loss in soft tissues caused by a trauma or a tumour requires a surgical reconstruction. Effective treatment of such defects can be prepared by tissue transplantation. Tissue engineering and regenerative medicine undergo significant development in the area of biomaterials and combination with stem cells offers accessible source for tissue reconstruction and transplantation (1–4). Biological cell-free material can serve as an optimal scaffold for wide applications as it does not evoke an immune response. Extracellular matrix (ECM) is a promising biomaterial alternative which provides a three-dimensional microenvironment niche for cells, which is highly specific for each type of tissue concerning the protein contents and complexity. There are several options how to substitute stromal components for scaffold production using: synthetic scaffold material, chemically cross-linked forms of ECM, purified ECM components or decellularization techniques. Successful decellularization produces biological material which combines advantages and properties of extracellular matrix as supportive microarchitecture, vascular network and participate in cell differentiation and proliferation (5, 6). Biological scaffolds composed of the extracellular matrix are commonly used in reconstructive surgical applications of many organs such as urinary bladder (7, 8), heart (9–11), lung (12, 13) or skin (14, 15).

This study compares decellularization effectiveness of two detergents, SDS (sodium dodecyl sulphate) and Triton X-100, which are both widely used as decellularization agents (16, 17). These agents supposed to maintain mechanical and structural integrity of the extracellular matrix with minimal damage of the scaffold, preserve vascular and neural networks and successfully remove nuclear and cytoplasmic components from ECM.

Material and Methods

All procedures were approved by the Ethical Committee supervising procedures on experimental animals at Charles University Medical Faculty in Hradec Králové.

Dissection of murine skeletal muscle tissue

A skeletal muscle tissue (approx. 1 × 0.5 × 0.5 cm pieces) was dissected from C57BL/6 mice and was immediately washed with PBS buffer and trimmed of a connective tissue and fat. The samples (n = 10) were fixed and processed for histological analysis.

Decellularization methods

We analysed two types of decellularization agents: 1% SDS (sodium dodecyl sulphate) and 1% Triton X-100 and samples were decellularized with the following protocol. Solutions were dissolved in distilled water.

A tissue was removed under aseptic conditions. Native samples were immediately processed after samples were delivered to the lab. The skeletal muscle was placed in 1% SDS or 1% Triton X-100 solution for 24 hours at room temperature under continuous shaking to remove cell components from the muscle tissue. The muscle sheets were

https://doi.org/10.14712/18059694.2017.36
© 2016 Charles University. This is an open-access article distributed under the terms of the Creative Commons Attribution License (http://creativecommons.org/licenses/by/4.0), which permits unrestricted use, distribution, and reproduction in any medium, provided the original author and source are credited.

thoroughly washed with the fresh PBS buffer for 24 h at 4 °C to wash out cells and potential SDS or Triton X-100 residues. The samples were used on the same day when they were prepared. All steps were processed in centrifuge tube with approx. 40 ml of solution.

Histological analysis

The specimens (untreated and decellularized scaffolds) were fixed in 10% formalin, embedded in paraffin and sectioned into 5 µm slices. Sections were deparaffinised, rehydrated and washed with distilled water. For histological analysis, the sections were stained with haematoxylin eosin, Sirius red, Alcian blue, lamina externa was impregnated by Jones' method, and elastic fibres were visualized with resorcin-fuchsin staining.

Results

Morphological characterization of physiological skeletal muscle

Native muscle samples were treated with two different decellularization agents and muscle morphology was examined with haematoxylin eosin staining compared to the untreated skeletal muscle sample. Figure 1A shows typical image of skeletal muscle represented by characteristic striated muscle fibres with nuclei localized beneath the sarcolemma revealing polygonal shape in a cross section.

Morphology of decellularized skeletal muscle tissue treated with SDS or Triton X-100 Haematoxylin eosin staining

SDS decellularization method resulted in a complete cell removal from the skeletal muscle tissue which was verified with standard haematoxylin-eosin staining. Tissue also revealed a general shrinkage. Microscopic architecture of the skeletal muscle tissue was preserved and typical polygonal shape of extracellular matrix, which surrounds empty spaces of striated skeletal fibres, was examined (Fig. 1B). Haematoxylin eosin staining revealed a complete removal of sarcoplasmic components which were washed out with PBS buffer. Three-dimensional architecture was preserved without nuclei remnants supported with DAPI staining showing no fluorescent signal (figure not shown).

Native skeletal muscle tissue treated with SDS revealed translucent composition; Triton X-100 did not have the same effect on the muscle tissue and remnants of unaffected tissue in the final scaffold could be observed.

Standard haematoxylin eosin staining proved presumption of inefficient decellularization based on Triton X-100 due to presence of some nuclei. Skeletal muscle fibres with occasional presence of striation were observed and presence of several nuclei underneath the sarcolemma (Fig. 1C) could

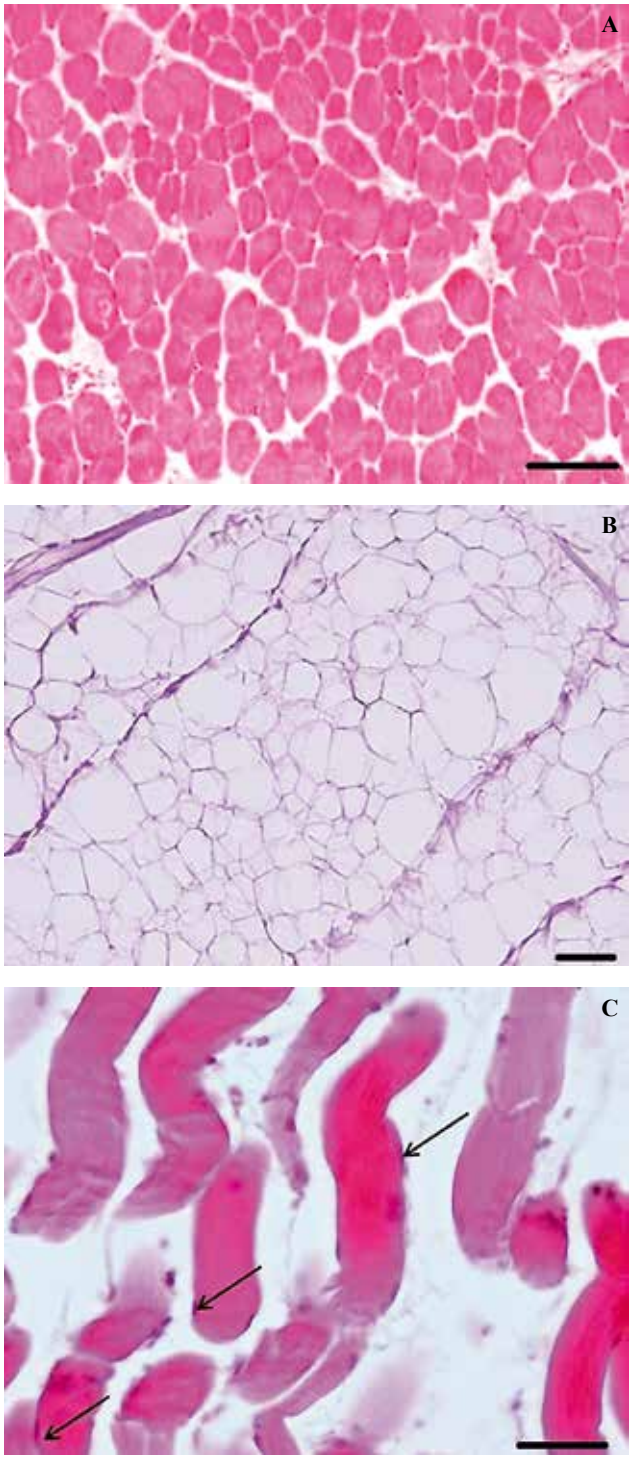

Fig. 1: Histological appearance after haematoxylin eosin staining of native muscle tissue (A) and muscle tissue treated with SDS (B) and Triton X-100 (C). Cross section of untreated muscle has typical architecture of skeletal muscle tissue while SDS-treated muscle shows disappearance of all cytoplasmic and nuclear components with preservation of ECM. Longitudinal section of a sample treated with Triton X-100 reveals presence of striated muscle fibres with preserved nuclei (arrows). Scale bar represents 50 µm.

be detected. Decellularization was inefficient, because ECM components were disrupted and debris surrounded striated muscle fibres DAPI staining showed positive fluorescent signal because of nuclei presence (figure not shown).

Sirius Red

Collagen structure is highly desirable to preserve after decellularization mainly for its structural function to sustain a shape of the scaffold. Sirius staining proved preservation of collagen in scaffold treated by SDS without any loss of collagen density or visible disruption of collagen fibres (Fig. 2A). Figure 2B showed another example of ineffective decellularization with Triton X-100; collagen fibres were heavily damaged and presence of striated muscle fibres was observed. Deterioration of collagen fibres caused lack of cohesion in scaffold and resulted in deformation of scaffold.

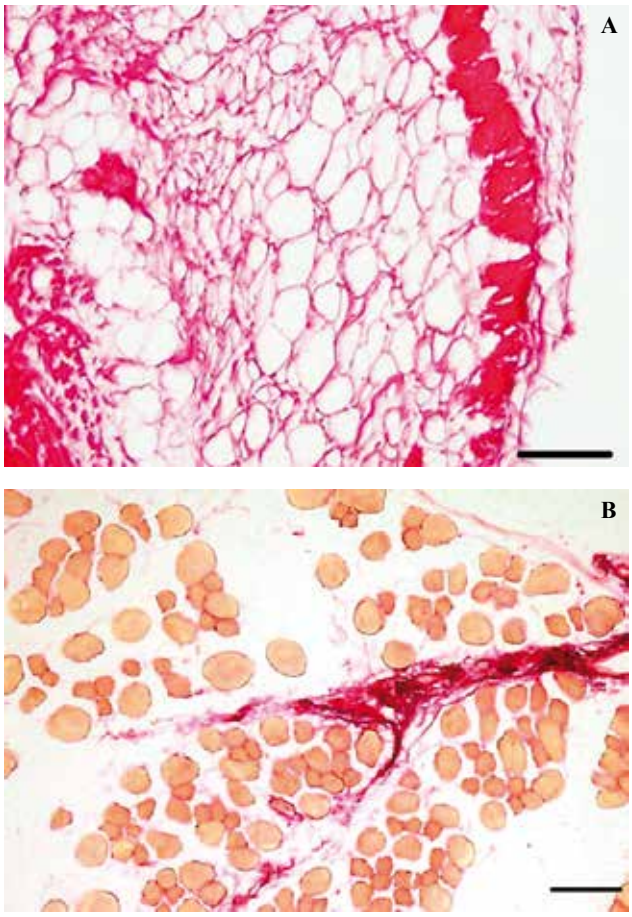

Fig. 2: Visualization of collagen fibres by Sirius Red staining in the skeletal muscle tissue decellularized by SDS (A) and Triton X-100 (B). Collagen fibres are stained deeply red as they are major components of ECM; high density of red staining in case of SDS treated tissue was observed. Triton X-100 decellularization preserved collagen fibres as well, but they lacked intactness and they were significantly reduced. Scale bar represents 50 µm.

Alcian blue staining

Alcian blue is a polyvalent basic dye for visualization of glycosaminoglycans (GAG) as a part of the ground substance which plays an important role in water retention and growth factor adhesion. SDS treatment preserved GAGs (Fig. 3A), but light blue staining probably illustrated a partial loss of these macromolecules. Nevertheless, glycosaminoglycans were preserved and intact. Decellularization by Triton X-100 preserved GAGs as well and a density of blue staining showed higher amount of GAGs in samples treated with Triton X-100 than in scaffolds decellularized by SDS. Glycosaminoglycans, presented in Triton X-100 scaffold, showed disruption and fragmentation.

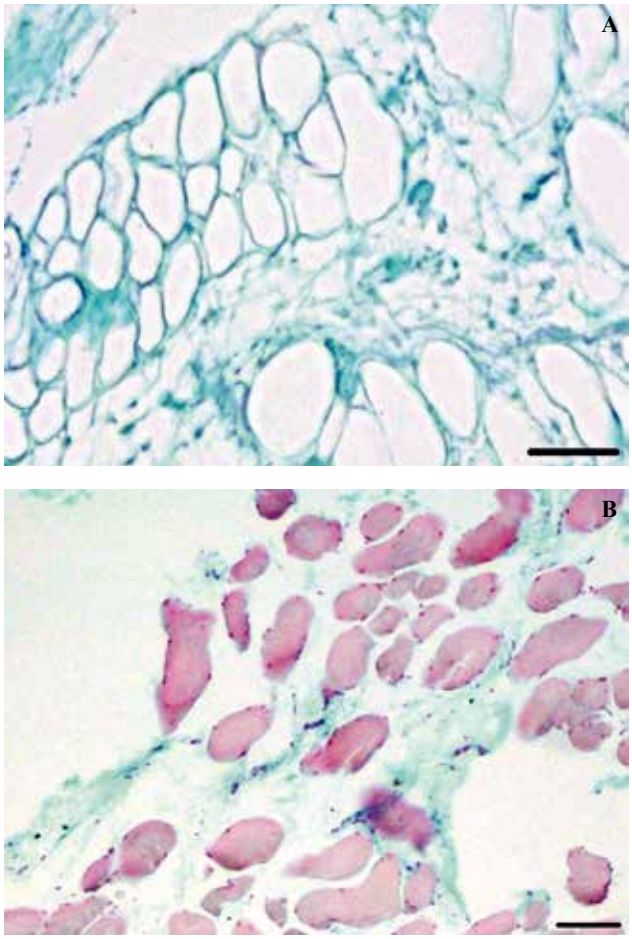

Fig. 3: Alcian blue staining illustrated presence of glycosaminoglycans in scaffold treated with SDS (A) or Triton X-100 (B). Scaffold prepared by SDS decellularization method demonstrates absence of striated muscle fibres and a typical honey-comb shape was preserved which is visualised by surrounding ECM, particularly blue coloured glycosaminoglycans. Triton treated samples also contained preserved glycosaminoglycans, but these scaffolds were unefficiently decellularized because of striated muscle fibres presence (pink stained structures with nuclei localized on the periphery, not shown in figure). Scale bar represents 50 µm.

Jones' impregnation method

Preservation of the lamina externa was determined with impregnation technique by Jones. The lamina externa is an essential component for cell attachment and tissue regeneration so it is crucial to preserve this structure. The lamina externa contains silver-reactive sites which surround adipocytes, peripheral nerve fibres and first of all muscle fibres. Decellularization had no severe effect upon lamina externa structure and both samples preserved this structure stained in black colour. Figure 4 shows impregnation of basement membrane which belongs to muscle fibres or to blood capillaries.

Resorcin-fuchsin staining

Elastic fibres are arranged in a branching pattern to form a three dimensional network and they are localized closely to collagen fibres to limit their distensibility of the tissue and prevent tearing from excessive stretching. No distortion or fragmentation was observed in case of a scaffold treated by SDS agens (Fig. 5A); elastic fibres were stained slightly lighter than in case of Triton X-100 decellularization. Triton X-100 scaffold stained with resorcin-fuchsin showed disruption of elastic fibres (Fig. 5B).

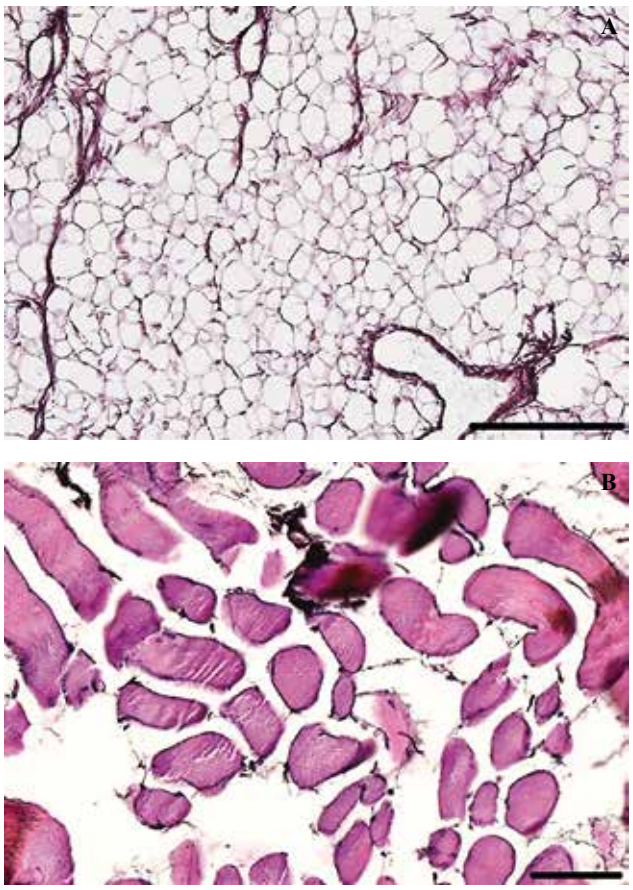

Fig. 4: Jones' impregnation revealed preservation of the basal lamina of decellularized samples processed by SDS (A) and Triton X-100 (B). Basement membrane is black coloured and surrounds former muscle fibres in case of SDS decellularization and partially lysed muscle fibres in Triton X-100 sample. Scale bar represents 50 µm.

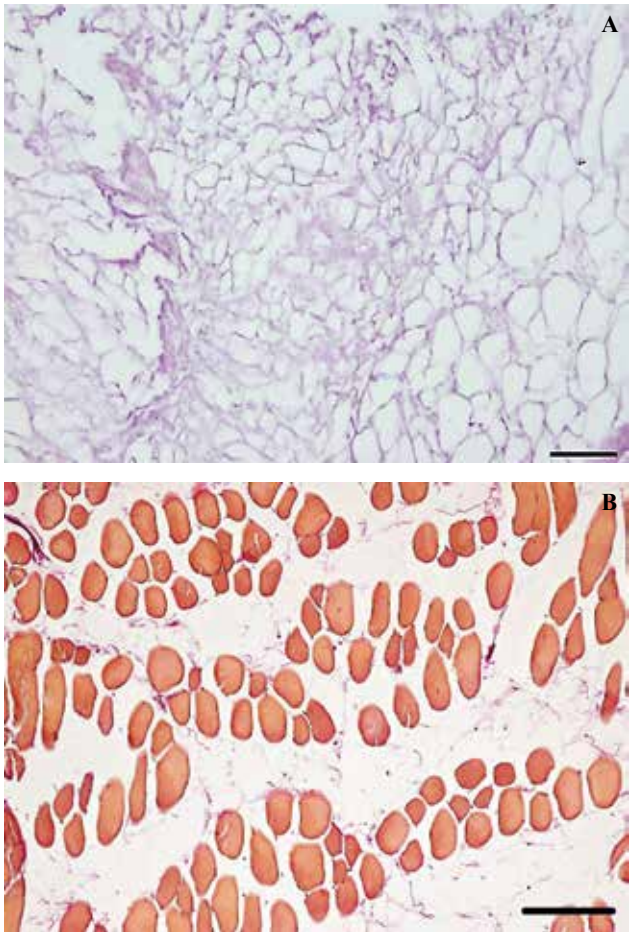

Fig. 5: Specific staining for elastic fibres, Resorcin-fuchsin, showed its preservation in samples decellularized by SDS (A) and Triton X-100 (B). Three dimensional network generated by elastic fibres was disrupted in case of Triton-decellularized samples which were visualised in violet colour, skeletal fibres by yellow to orange colour. Preserved nuclei were observed in Figure 5B and surrounding extracellular matrix changed according to its damage caused by Triton effect and a whole tissue had alternated microarchitecture. This architecture damage can be compared with the scaffold prepared by SDS decellularization (A) which preserved three dimensional network and all cytoplasmic and nuclear components were absent in this scaffold. Scale bar represents 50 µm.

Discussion

The main goal of this study was to clarify efficiency of two decellularization agents, SDS and Triton X-100, which

are both the most used detergents to produce tissue or organ scaffolds. Effective decellularization process has minimal effect on the extracellular matrix, preserves a three dimensional microarchitecture of a tissue as a scaffold for tissue or organ reconstruction and most of all eliminates cellular material from the tissue. To verify effectiveness of individual decellularization agents, we analysed scaffolds with several histological techniques which evaluate ability of Triton X-100 and SDS to eliminate cell nuclei and preserve main ECM components, such as collagen, glycosaminoglycans, basal lamina and elastic fibres.

Our idea to compare influence of Triton X-100 and SDS was based on studies (18–20) which used these two agents to prepare decellularized scaffolds. Both of these agents disrupt the cell membrane causing cell lysis by osmotic gradient. Detergents are effective in a cell removal from in the scaffold which can have a crucial role in an immune response, but they also can affect negatively structure of the scaffold; for instance, Triton X-100 can affect a decrease of GAG and damage ultrastructure of tissue or organ (21, 22). SDS also removes effectively cell nuclei and cytoplasmic components, especially from dense tissues, but they tend to damage collagen and decrease GAG content (23, 24), so they have very similar adverse consequence on the extracellular matrix. As both these agents are considered to be effective decellularization reagents, we would like to know which one is more effective in decellularizing the skeletal muscle tissue and for that reason we choose the same conditions in decellularization protocol (including length of decellularization, material and technique to apply the agent).

After decellularization, the skeletal muscle tissue appeared almost translucent in SDS protocol; Triton protocol did not affect a muscle so well and we could observe cytoplasmic debris in the tissue. Overall, our study proved higher efficiency of SDS agent to decellularize the skeletal muscle tissue which was supported by several histological findings. Haematoxylin eosin, as a standard method for the first tissue inspection, showed persistence of striated muscle fibres and nuclei after treatment with Triton X-100 which is according to criteria stated by Gilbert and Crapo (25) (lack of visible nuclear and cytoplasmic material in tissue section stained with haematoxylin and eosin staining) considered as ineffective decellularization. Elimination of cells from tissue or organ is crucial for subsequent implantation of the scaffold into living organism and significantly decreases a risk of rejection.

The extracellular matrix is a complex of structural and functional proteins and each type of tissue has specific composition of these proteins (26). The most abundant ECM protein is collagen which is present in several motifs as collagen type IV in basal membrane of vascular structures, collagen type I in collagen fibres, collagen type VII as an anchoring fibrils. Preservation of a different type of collagen was evaluated by two methods as Sirius Red method and Jones' impregnation. Sirius Red is specific staining method to distinguish collagen fibres, especially it allows determining difference between collagen type I and III. This type of staining revealed no changes in collagen distribution after SDS cell extraction, either fragmentation or distortion. These results were not observed in Triton X-100 treatment; collagen fibres were unevenly distributed in ECM and were heavily damaged which could cause incoherence and mechanical endurance of tissue or organ. Triton protocol also decreased collagen density as reported in the study by Graus et al. (27). Elastin fibres accompany collagen fibres and are arranged in a branching pattern forming a three dimensional network. These fibres play an important role in distensibility of the tissue and can prevent tearing from stretching. SDS and Triton X-100 treatment of the skeletal muscle tissue preserved elastin fibres, but Triton X-100 damaged fibres morphology and altered molecular structure of elastin resulting in uneven distribution of elastic fibres. SDS decellularization affects elastin fibres in content which was decreased. Laminin, collagen type IV and anchoring fibrils are the most prominent structures in basement membrane and they specify its ultrastructure and function as an attachment site for cells, filtration, and regulation and also provide scaffold during regeneration (28). Decellularized samples processed from both decellularized agents revealed intactness of basement membrane as visualized by Jones' impregnation.

The ability of preserving glycosaminoglycans was also compared in both skeletal muscle tissues treated by SDS and Triton X-100. SDS decellularization protocol successfully retains these heteropolysaccharides which are bound to proteoglycans and serve as binding sites for growth factors, cytokines and contribute to water retention due to their negative charge (29). Triton X-100 treatment results in significant elimination of GAGs from the skeletal muscle tissue as analysed by Alcian blue staining. Reduced content of GAGs in the scaffold may decrease mechanical resistance because of GAGs are responsible for gel consistency which can resist deformations during tissue function (24, 28). Decellularization with SDS as a main agent was more successful in term of GAGs preservation, but amount of these macromolecules was also decreased. These results are consistent with other studies (30, 21) using SDS as a main decellularization agent.

Conclusion

ECM alteration or damage can be caused during decellularization by several factors including type of used detergent, concentration of detergent, duration of decellularization process, presence of protease inhibitor etc. (31). Differences between various decellularization agents are based upon their function and these variations determine discrepancies in effect on the extracellular matrix. Our study proves that ionic detergent SDS is sufficient agent for cells removal in the skeletal muscle tissue and preservation of the extracellular matrix microarchitecture providing microenvironment suitable for cell attachment and growth.

Acknowledgements

This work was supported by the Grant Agency of the Czech Republic 15-09161S, Grant of the Charles University No. SVV-2016-260278 and PRVOUK P37/06.

Abbreviation

ECM extracellular matrix
DAPI 4′,6-diamidino-2-phenylindole
GAG glycosaminoglycans
PBS phosphate buffered saline
SDS sodium dodecyl sulphate

References

1. Cheng CW, Solorio LD, Alsberg E. Decellularized tissue and cell-derived extracellular matrices as scaffolds for orthopaedic tissue engineering. Biotechnol Adv 2014; 32: 462–84.
2. Hurd SA, Bhatti NM, Walker AM, Kasukonis BM, Wolchok JC. Development of a biological scaffold engineered using the extracellular matrix secreted by skeletal muscle cells. Biomaterials 2015; 49: 9–17.
3. Wang L, Johnson JA, Chang DW, Zhang Q. Decellularized musculofascial extracellular matrix for tissue engineering. Biomaterials 2013; 34: 2641–54.
4. Criswell TL, Corona BT, Wang Z et al. The role of endothelial cells in myofiber differentiation and the vascularization and innervation of bioengineered muscle tissue in vivo. Biomaterials 2013; 34: 140–9.
5. Yamamoto K, Murphy G, Troeberg L. Extracellular regulation of metalloproteinases. Matrix Biol 2015; 44–46: 255–63.
6. Schultz GS, Wysocki A. Interactions between extracellular matrix and growth factors in wound healing. Wound Repair Regen 2009; 17: 153–62.
7. Reddy PP, Barrieras DJ, Wilson G et al. Regeneration of functional bladder substitutes using large segment acellular matrix allografts in a porcine model. J Urol 2000; 164: 936–41.
8. Rosario DJ, Reilly GC, Salah EA, Glover M, Bullock AJ, MacNeil S. Decellularization and sterilization of porcine urinary bladder matrix for tissue engineering in the lower urinary tract. Regen Med 2008; 3: 145–56.
9. Quarti A, Nardone S, Colaneri M, Santoro G, Pozzi M. Preliminary experience in the use of an extracellular matrix to repair congenital heart diseases. Interact Cardivasc Thorac Surg 2011; 6: 659–72.
10. Dong J, Li Y, Mo X. The study of a new detergent (octyl-glucopyranoside) for decellularizing porcine pericardium as tissue engineering scaffold. J Surg Res 2013; 183: 56–67.
11. Weber B, Dijkman PE, Scherman J et al. Off-the-shelf human decellularized tissue-engineered heart valves in a non-human primate model. Biomaterials 2013; 34: 7269–80.
12. Nonaka PN, Uriarte JJ, Campillo N et al. Mechanical properties of mouse lungs along organ decellularization by sodium dodecyl sulfate.Respir Physiol Neurobiol 2014; 200: 1–5.
13. O'Neill JD, Anfang R, Anandappa A et al. Decellularization of human and porcine lung tissues for pulmonary tissue engineering. Ann Thorac Surg 2013; 96: 1046–55.
14. Gupta SK, Dinda AK, Potdar PD, Mishra NC. Fabrication and characterization of scaffold from cadaver goat-lung tissue for skin tissue engineering applications. Mater Sci Eng C Mater Biol Appl 2013; 33: 4032–8.
15. Su Z, Ma H, Wu Z et al. Enhancement of skin wound healing with decellularized scaffolds loaded with hyaluronic acid and epidermal growth factor. Mater Sci Eng C Mater Biol Appl 2014; 44: 440–8.
16. Baptista MP, Siddiqui MM, Lozier G, Rodriguez SR, Atala A, Soker S. The use of whole organ decellularization for the generation of a vascularized liver organoid. Hepatology 2011; 53: 604–17.
17. Ott CH, Mathiesen TS, Goh SK et al. Perfusion-decellularized matrix: using nature's platform to engineer a bioartificial heart. Nature Medicine 2007; 14: 213–21.
18. Ungerleider JL, Johnson TD, Rao N, Christman KL. Fabrication and characterization of injectable hydrogels derived from decellularized skeletal and cardiac muscle. Methods 2015; 84: 53–9.
19. Perniconi B, Costa A, Aulino P, Teodori L, Adamo S, Coletti D. The pro-myogenic environment provided by whole organ scale acellular scaffolds from skeletal muscle. Biomaterials 2011; 32: 7870–82.
20. Caralt M, Uzarski JS, Iacob S et al. Optimization and critical evaluation of decellularization strategies to develop renal extracellular matrix scaffolds as biological templates for organ engineering and transplantation. Am J Transplant 2015; 15: 64–75.
21. Ott HC, Matthiesen TS, Goh SK et al. Perfusion decellularized matrix: using nature's platform to engineer a bioartificial heart. Nat Med 2008; 14: 213–21.
22. Uygun BE, Soto-Gutierrez A, Yagi H et al. Organ reengineering through development of a transplantable recellularized liver graft using decellularized liver matrix. Nat Med 2010; 16: 814–20.
23. Reing JE, Brown BN, Daly KA et al. The effects of processing methods upon mechanical and biologic properties of porcine dermal extracellular matrix scaffolds. Biomaterials 2010; 31: 8626–33.
24. Du L, Wu X, Pang K, Yang Y. Histological evaluation and biomechanical characterisation of an acellular porcine cornea scaffold. Br J Ophthalmol 2011; 95: 410–4.
25. Crapo PM, Gilbert TW, Badylak SF. An overview of tissue and whole organ decellularization processes. Biomaterials 2011; 32: 3233–43.
26. Hrebikova H, Diaz D, Mokry J. Chemical decellularization: a promising approach for preparation of extracellular matrix. Biomed Pap Med Fac Univ Palacky Olomouc Czech Repub 2015; 159: 12–7.
27. Grauss RW, Hazekamp MG, Oppenhuizen F, Munsteren CJ, Gittenberger-de Groot AC, DeRuiter MC. Histological evaluation of decellularized porcine aortic valves: matrix changes due to different decellularization methods. Eur J Cardiothorac Surg 2005; 27: 566–71.
28. Ross MH, Pawlina W. Histology, text and atlas: with correlated cell and molecular biology. 6th ed. Philadelphia: Wolter Kluwer, 2011.
29. Badylak SF. Xenogeneic extracellular matrix as a scaffold for tissue reconstruction. Transpl Immunol 2004; 12: 367–77.
30. Gilpin SE, Guyette JP, Gonzalez G et al. Perfusion decellularization of human and porcine lungs: bringing the matrix to clinical scale. J Heart Lung Transplant 2014; 33: 298–308.
31. Gilbert TW, Sellaro TL, Badylak SF. Decellularization of tissues and organs. Biomaterials 2006; 27: 3675–83.

Received: 03/08/2016
Accepted: 19/10/2016

ORIGINAL ARTICLE

Clinical Study of 23 Male Patients with Congenital Ventral Penile Angulation without Hypospadias

Ioannis Patoulias, Dimitrios Patoulias, Konstantinos Farmakis, Maria Kalogirou*

1st Department of Pediatric Surgery, Aristotle University of Thessaloniki, GH G. Gennimatas, Thessaloniki, Greece
* Corresponding author: M. Alexandrou 3B, Peuka, Thessaloniki, Postal code 57010; e-mail address: dipatoulias@gmail.com

Summary: Congenital ventral penile angulation without hypospadias is a rare disease and causes great anxiety to the parents. The aim of our study is the presentation of this disease, especially the indications of surgical treatment and the protocol applied in our clinic. We retrospectively studied 23 male patients aged 2.5 to 7 years old (av 5.2 y) with important penile angulation (over 45°) without hypospadias, treated during the past 15 years in our department. In 9 patients the cause was the skin chordee (fibrosis of the ventral part of the prepuce), in 4 the fibrotic fascia (incomplete development of dartos and Buck's fascia) and in 10 the disproportion of the corpora cavernosa. No case of congenital short urethra was reported. In our opinion, the appliance of the algorithm suggested by Donnahoo KK et al. in uncomplicated cases, along with the experience of the surgical team, results in satisfactory treatment and avoidance of complications.

Keywords: *Penile angulation without hypospadias; Chordee; Male child; Short urethra*

Introduction

Penile angulation without hypospadias is a stage of penile development at 16th week of gestation, which gradually disappears from 20th to 25th week (1). It can remain in one third of premature neonates and disappears during the first months of life. Congenital penile angulation without hypospadias (CPAwH) less than 45° is reported in 4–10% of boys (2). It is usually first observed by the parents.

Incidence of severe CPAwH in Danish children as estimated by Ebbehøj and Metz is 0.37/1000 boys (3). Yachia D applied a vacuum induced erection system, concluding that the incidence rises up to 0.6% of boys (4, 5).

CPAwH with ventral curvature is the most often subtype and concerns about 84% of all cases, while dorsal (11%) and lateral curvature (5%) are less frequent (6). Surgical treatment is indicated when ventral curvature exceeds 45° (7).

The aim of our study is to illustrate this rare disease, the surgical indications and the treatment protocol applied in our clinic.

Material and Methods

During the last 15 years in the 1st Department of Pediatric Surgery, Aristotle University of Thessaloniki we treated 23 boys aged from 2.5 to 7 years old (average 5.2 y), with congenital penile angulation more than 45°, without hypospadias. We applied the following algorithm, suggested by Donnahoo KK et al (8) (Table 1):

A. Erection test (Figure 1) in order to estimate the degree of the angulation (Gittes and McLaughlin technique) (9).
B. Degloving of the penis after performing a subcoronal circumferential skin incision up to the Buck's fascia and repetition of the erection test. If a straightening of the penis is achieved, we transfer a skin flap from the dorsal to the ventral surface of the penis (button hole or Byars flaps). This transfer is also applied after successful straightening in the following steps.
C. If the angulation persists, excision of the fibrous tissue (malformated dartos and deep fascia of the penis) of the ventral penile surface follows.
D. In cases of still persisting angulation, we conduct a tunica albuginea plication in the position of the greatest curvature. In cases of significant angulation, we place a skin graft on the ventral surface of the corpora cavernosa.
E. In a angulation persists due to a urethral tendering-short urethra, urethral mobilization is needed, combined with construction of neourethra if needed.
F. If the angulation is caused by the disproportion of the corpora cavernosa (corporal rotation and penile disassembly), we longitudinally separate a) the corpus cavernosum from the corpus spongiosum of the urethra starting from the level of the glans and b) the intracavernosal septum. During this procedure, folding of the tunica albuginea of the longer corpus cavernosum respectively to its lateral surface may be needed.

As mentioned above, the operation is completed with the transfer of a skin flap from the dorsal to the ventral surface of the penis.

https://doi.org/10.14712/18059694.2017.37
© 2016 Charles University. This is an open-access article distributed under the terms of the Creative Commons Attribution License (http://creativecommons.org/licenses/by/4.0), which permits unrestricted use, distribution, and reproduction in any medium, provided the original author and source are credited.

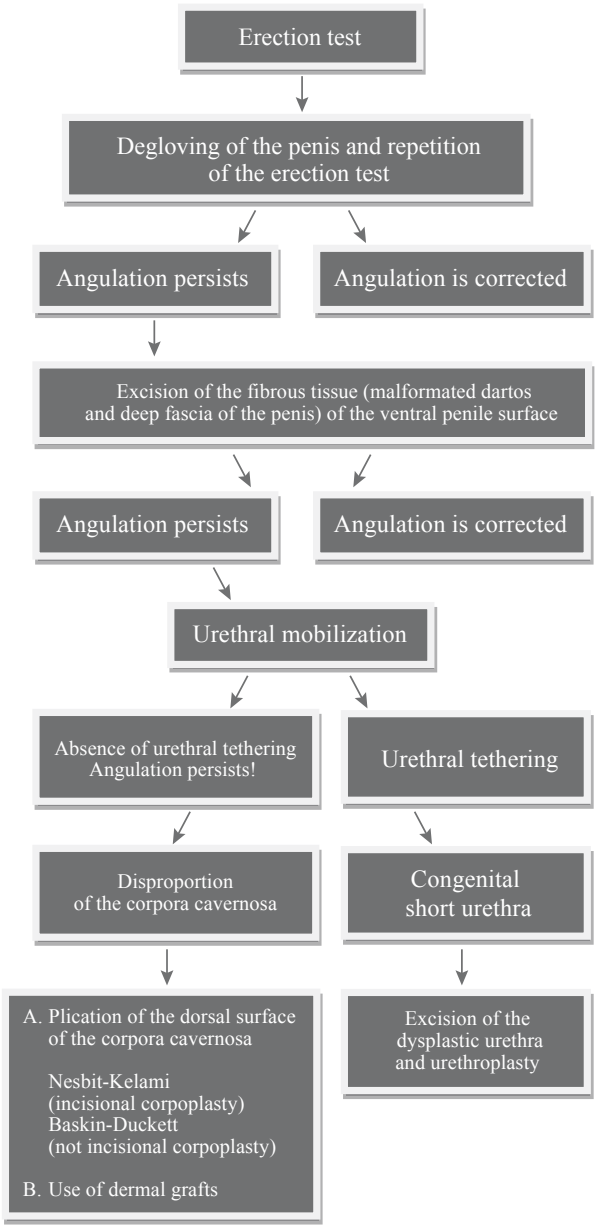

Tab. 1: Algorithm of surgical approach of congenital ventral penile angulation without hypospadias, suggested by Donnahoo KK et al. (8).

Results

We divided our patients into three groups according to the surgical findings: Group A included 9 patients on which straightening of the penis was achieved by degloving. In Group B, which included 4 patients, excision of the fibrous tissue (malformated dartos and Buck's fascia) from the ventral surface of the penis was conducted. In group C, 10 patients needed a plication of the dorsal surface of the corpora cavernosa. In 6 patients of group C we used

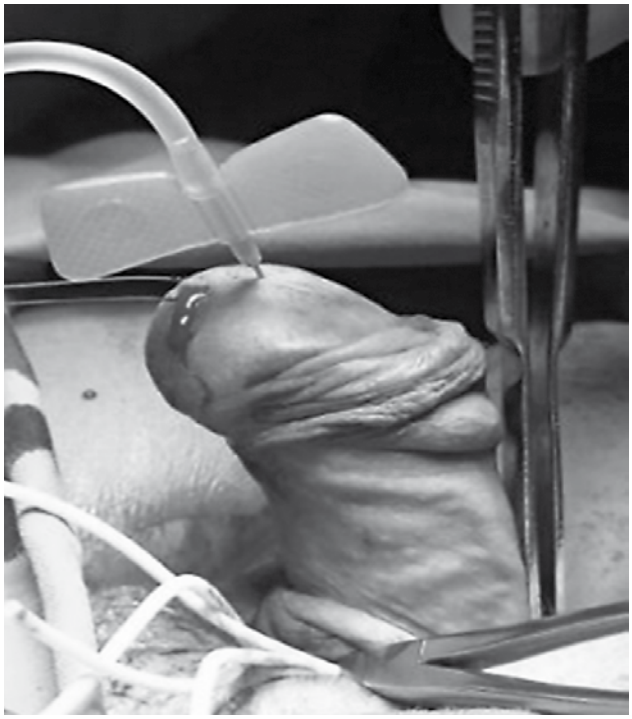

Fig. 1: Erection test. 45° ventral penile angulation (second patient of group A).

the Nesbit technique and in 4 patients of the same group the Baskin-Duckett technique.

No postoperative complications were reported. The urethral catheter was removed the 2nd post-op day. Total hospitalization lasted 3–4 days. The moderate edema of the prepuce decreased in the first ten days. In all three groups, the results seven years after the surgical procedure were evaluated as satisfactory (without relapse of the angulation and with penile length within the normal range for the patient's age) and well accepted by parents.

Discussion

In 1973 Divine and Horton (10) were the first authors that classified CPAwH in three types according to etiology. Type I concerns about a complex malformation of the corpus spongiosum, the Buck's fascia and the dartos. Type II concerns about the Buck's fascia and the dartos and type III only about dartos. A type IV was added 2 years later by Kaplam and Lamm, which is about a disproportion between the dorsal and the ventral surface of the corpora cavernosa (1). A report over type IV was described 7 years later by Kramer, Aydin and Kelalis (2). In 1991 Devine and Blackley et al (11) described a type V induced by a congenital short urethra or the existence of a fibrous chordee dorsally of the urethra's corpus spongiosum. Type V is not fully accepted (7, 12, 13). According to Snodgrass WT (7), type V could be classified as hypospadias variant in the future.

Donnahoo and Chain et al (8), after studying 87 cases, tried to create an updated classification of CPAwH (Table 2). In our study 9 patients come under type I (38%), 4 under type 2 (18%), 10 under type III (44%), while there were no patients with type IV of CPAwH.

Tab. 2: Etiology classification of CPAwH by Donnahoo and Chain et al.

Type	Cause	%
I	Lack of flexibility of the ventral surface of the prepuce	32
II	Fibrosis-malformation of dartos and Buck's fascia	33
III	Disproportion between the dorsal and the ventral surface of the corpora cavernosa	28
IV	Congenital short urethra	7

The aim of surgical intervention is the creation of a straightened penis during erection, without a proximal transposition of the external urethral orifice, decrease in the penis' length or damage at its structures (corpora cavernosa, urethra, neurovascular bundle complex).

Degloving of the penis was achieved. During the excision of the malformative fibrous tissue (group B) respectively to the ventral penile surface respectively at the level of the dartos, we paid extra attention in order to preserve the corpus spongiosum of the urethra and avoid complications. In group C we applied incisional corpoplasty (Nesbit's technique) in 6 patients and plicational corpoplasty (Baskin-Duckett's technique) in 4 patients. Using the Nesbit's technique, we incised the fibrous layer in the points of the greatest curvature (along the 11 to 1 o'clock position of the penis), in order to preserve the neurovascular bundle complex (14, 15, 16).

In order to estimate the accurate number of needed incisions, we followed the principles described by Kelami (14). Before those incisions, we grasped the fibrous layer of the corpora cavernosa using Allis clamps and then conducted the erection test. Provided the desirable result, we incised and sutured the fibrous layer transversally with PDS 3/0 and the knots on the inside of the incision. Plication of the fibrous layer was conducted in 4 patients. Selection of each technique was made by each surgeon. No recurrence caused by sutures transversing the fibrous layer was noticed.

If – in the context of surgical procedure – an extended intervention in the corpora cavernosa is required, this can lead either to a recurrence of the angulation with dorsal orientation or – during the development of the patient – to an iatrogenic shortening of the corpora cavernosa. In this case, it is indicated to make an incision in the ventral surface of corpora cavernosa, respectively to the opposite position of the greatest curvature, and to place skin grafts. Badaway and Morsi evaluated 16 patients who underwent this technique, 10 years later, and found that 14/16 of them had an aligned penis during erection (17).

In cases of short or dysplastic urethra treatment options are:

1. Resection of hypoplastic urethra, excision of underlying fascial tissue and replacement urethroplasty (18, 19, 20).
2. Division of the mid-portion of hypoplastic urethra and replacement by using a tubularized or island flap or Asopa skin tube (18, 19, 20, 21).
3. Mobilization of hypoplastic urethra and spongioplasty: divergent (Y-shaped) corpus spongiosum along with the hypoplastic urethra, starting from the normal urethra to the tip of glans (22).

If one of the above is applied, but the CPAwH persists, then penile disassembly might be an alternative therapeutic option (23).

Singh S. et al. (21) encountered 26 patients with CPAwH, with successful outcome rising up to 65.6% of all cases. According to the authors, their results were poorer comparing to those of Donnahoo et al. (8) due to the fact that in their clinical study hypoplastic or dysgenic urethra co-existed in a higher proportion (65.38% vs. 7% in Donnahoo's study). They also suggest an interesting classification of the disease based on operative findings. Thus, in our opinion, it plays a significant and catalytic role for the pediatric surgeons in the stepwise management of more complex cases of CPAwH.

We believe that using the algorithm suggested by Donnahoo KK et al. (8), successful treatment without complications can be achieved, especially in the mild to moderate forms of CPAwH. We did not confront serious complications – such as the remaining of the chordee or a fistula –, which are reported in current literature at a rate 7–8% in the groups A–C and 50% in group D. The absence of patients with type IV CPAwH (dysplastic or short urethra) in our study group led partially to the lower rate of complications.

Conclusions

1. CPAwH is a rare penile anomaly, cause of great anxiety for the parents. If it is greater than 45 degrees, it must be surgically corrected.
2. Ventral surface of the prepuce, dartos and Buck's fascia are usually involved in its formation.
3. Penile degloving, excision of the malformated fibrous tissue of the ventral surface of the prepuce and straightening of the dorsal surface of the fibrous layer of the corpora cavernosa are sufficient, in order to correct the angulation in 65–92% of the cases (14).

Conflict of interest

None of the contributing authors have any conflict of interest, including specific financial interests or relationships and affiliations relevant to the subject matter or materials discussed in the manuscript.

References

1. Kaplan GW, Lamm DL. Embryogenesis of chordee. J Urol 1975; 114: 769–72.
2. Kramer S, Aydin G, Kelalis P. Chordee without hypospadias in children. J Urol 1982; 128: 559–61.
3. Ebbehøj J, Metz P. Congenital penile angulation. Br J Urol 1987; 60: 264–6.
4. Yachia D. Early assessment of penile curvatures in infants. J Urol 1991; 145: 103–4.
5. Yachia D, Beyar M, Aridogan IA, et al. Incidence of penile curvatures. J Urol 1993; 150: 1478–9.
6. Zachalski W, Krajka K, Matuszewski M. Evaluation of the Treatment of Congenital Penile Curvature Including Psychosexual Assessment. J Sex Med 2015; 12(8): 1828–35.
7. Snodgrass WT. Management of penile curvature in children. Current Opinion in Urology 2008; 18(4): 431–5.
8. Donnahoo KK, Cain MP, Pope JC, et al. Etiology, management and surgical complications of congenital chordee without hypospadias. J Urol 1998; 160: 1120–2.
9. Gittes RF, McLoughlin AP 3rd. Injection technique to induce penile erection. Urology 1974; 4: 473–4
10. Devine CJ Jr., Horton CE. Chordee without hypospadias. J Urol 1973; 110(2): 264–71.
11. Devine CJ Jr., Blackley SK, Horton CE, Gilbert DA.The surgical treatment of chordee without hypospadias in men. J Urol 1991; 146: 325–8.
12. Baskin LS, Erol A, Li YW, et al. Anatomical studies of hypospadias. J Urol 1998; 160: 1108–15.
13. Montag S, Palmer LS, Abnormalities of penile curvature: chordee and penile torsion, ScientificWorldJournal. 2011 Jul 28; 11: 1470–8.
14. Kelami A. Congenital penile deviation and its treatment with Nesbit-Kelami technique. Br J Urol 1987; 60: 261–3.
15. Van Der Horst C, Martínez Portillo FJ, Seif C, et al. Treatment of penile curvature with Essed-Schröder tunical plication: aspects of quality of life from the patients' perspective. BJU Int 2004; 93(1): 105–8.
16. Tang Y-M, Chen S-J, Huang L-G, et al.: Chordee without Hypospadias: Report of 79 Chinese Prepubertal Patients. J Androl 2007; 28(4): 630–3.
17. Badawy H, Morsi H. Long-Term Follow up of Dermal Grafts for Repair of Severe Penile Curvature. J Urol 2008; 180(4): 1842–5.
18. Daskalopoulos EI, Baskin L, Duckett JW, et al. Congenital penile curvature (chordee without hypospadias). Urology 1993; 42(6): 708–12.
19. Bhat A, Sabharwal K, Bhat M, et al., Correction of penile torsion and chordee by mobilization of urethra with spongiosum in chordee without hypospadias, J Pediatr Urol 2014; 10(6): 1238–43.
20. Bhat A, Saxena G, Abrol N. A new algorithm for management of chordee without hypospadias based on mobilization of urethra. J Pediatr Urol 2008; 4(1): 43–50.
21. Singh S, Rawat J, Kureel SN et al. Chordee without hypospadias: Operative classification and its management. Urol Ann 2013; 5(2): 93–8.
22. Jednak R, Hernandez N, Spencer Barthold J, et al. Correcting chordee without hypospadias and with deficient ventral skin: a new technique. BJU Int 2001; 87(6): 528–30.
23. Perovic SV, Djordjevic ML, Djakovic NG, A new approach to the treatment of penile curvature. J Urol 1998; 160(3 Pt 2): 1123–7.

Received: 02/09/2016
Accepted: 20/10/2016

ORIGINAL ARTICLE

Common mistakes in the Dual-Energy X-ray Absorptiometry (DXA) in Turkey. A Retrospective Descriptive Multicenter Study

Ali Yavuz Karahan[1,], Bugra Kaya[2], Banu Kuran[3], Ozlem Altındag[4], Pelin Yildirim[5], Sevil Ceyhan Dogan[6], Aynur Basaran[1], Ender Salbas[7], Turgay Altınbilek[8], Tuba Guler[5], Sena Tolu[9], Zekiye Hasbek[10], Banu Ordahan[1], Ercan Kaydok[11], Ufuk Yucel[11], Selcuk Yesilyurt[12], Almula Demir Polat[13], Murat Cubukcu[14], Omer Nas[15], Umit Sarp[15], Ozan Yasar[16], Seher Kucuksarac[1], Gozde Turkoglu[1], Ahmet Karadag[17], Sinan Bagcaci[18], Kemal Erol[19], Emel Guler[20], Serpil Tuna[21], Ahmet Yildirim[22], Savas Karpuz[1]*

[1] Department of Physical Medicine and Rehabilitation, Beyhekim State Hospital of Konya Konya/Turkey
[2] Department of Nuclear Medicine of Necmettin Erbakan University, Meram Faculty of Medicine Konya/Turkey
[3] Department of Physical Medicine and Rehabilitation, Sisli Etfal Training and Research Hospital Istanbul/Turkey
[4] Department of Physical Medicine and Rehabilitation, Gaziantep University Sahinbey Research and Training Hospital, Gaziantep/Turkey
[5] Department of Physical Medicine and Rehabilitation, Derince Training and Research Hospital Kocaeli/Turkey
[6] Department of Physical Medicine and Rehabilitation, Cumhuriyet University, Faculty of Medicine Sivas/Turkey
[7] Department of Physical Medicine and Rehabilitation, State Hospital of Agri/Turkey
[8] Department of Physical Medicine and Rehabilitation, Physical therapy High school of Health Sciences of University of Halic, Istanbul/Turkey
[9] Department of Physical Medicine and Rehabilitation, Medipol University, Faculty of Medicine Istanbul/Turkey
[10] Department of Nuclear Medicine, Cumhuriyet University, Faculty of Medicine Sivas/Turkey
[11] Department of Physical Medicine and Rehabilitation, State Hospital of Nevsehir/Turkey
[12.] Department of Physical Medicine and Rehabilitation, Physical Medicine and Rehabilitation Hospital of Yoncali, Kutahya/Turkey
[13] Department of Physical Medicine and Rehabilitation, State Hospital of Afyon/Turkey
[14] Department of Physical Medicine and Rehabilitation, State Hospital of Denizli/Turkey
[15] Department of Physical Medicine and Rehabilitation, State Hospital of Yozgat/Turkey
[16] Department of Physical Medicine and Rehabilitation, Amasya University Sabuncuoglu Serefeddin Research and Training Hospital, Amasya/Turkey
[17] Department of Physical Medicine and Rehabilitation, State Hospital of Sivas/Turkey
[18] Department of Physical Medicine and Rehabilitation, State Hospital of Hakkari/Turkey
[19] Department of Physical Medicine and Rehabilitation, State Hospital of Nigde/Turkey
[20] Department of Physical Medicine and Rehabilitation, Kayseri Training and Research Hospital Kayseri/Turkey
[21] Department of Physical Medicine and Rehabilitation, Akdeniz University, Faculty of Medicine Antalya/Turkey
[22] Department of Orthopedics and Traumatology, Beyhekim State Hospital of Konya Konya/Turkey
* Corresponding author: Department of Physical Medicine and Rehabilitation, State Hospital of Konya/Turkey, Yunusemremhnuranşsk no1 meramkonya; e-mail: ayk222@hotmail.com

Summary: Background: Osteoporosis is a widespread metabolic bone disease representing a global public health problem currently affecting more than two hundred million people worldwide. The World Health Organization states that dual-energy X-ray absorptiometry (DXA) is the best densitometric technique for assessing bone mineral density (BMD). DXA provides an accurate diagnosis of osteoporosis, a good estimation of fracture risk, and is a useful tool for monitoring patients undergoing treatment. Common mistakes in BMD testing can be divided into four principal categories: 1) indication errors, 2) lack of quality control and calibration, 3) analysis and interpretation errors, and 4) inappropriate acquisition techniques. The aim of this retrospective multicenter descriptive study is to identify the common errors in the application of the DXA technique in Turkey. Methods: All DXA scans performed during the observation period were included in the study if the measurements of both, the lumbar spine and proximal femur were recorded. Forearm measurement, total body measurements, and measurements performed on children were excluded. Each examination was surveyed by 30 consultants from 20 different centers each informed and trained in the principles of and the standards for DXA scanning before the study. Results: A total of 3,212 DXA scan results from 20 different centers in 15 different Turkish cities were collected. The percentage of the discovered erroneous measurements varied from 10.5% to 65.5% in the lumbar spine and from 21.3% to 74.2% in the proximal femur. The overall error rate was found to be 31.8% (n = 1021) for the lumbar spine and 49.0% (n = 1576) for the

https://doi.org/10.14712/18059694.2017.38
© 2016 Charles University. This is an open-access article distributed under the terms of the Creative Commons Attribution License (http://creativecommons.org/licenses/by/4.0), which permits unrestricted use, distribution, and reproduction in any medium, provided the original author and source are credited.

proximal femur. Conclusion: In Turkey, DXA measurements of BMD have been in use for over 20 years, and examination processes continue to improve. There is no educational standard for operator training, and a lack of knowledge can lead to significant errors in the acquisition, analysis, and interpretation.

Keywords: *Osteoporosis; Dıagnosis; Dual Energy X-ray Absorptiometry; Technician; Education*

Introduction

Bone mineral density (BMD) is used in clinical practice as an indirect indicator of osteoporosis and fracture risk (1). Bone densitometry has quickly become the internationally accepted in-vivo bone mass measurement (1–3). The modalities of bone densitometry instruments include dual-energy X-ray absorptiometry (DXA), quantitative ultrasound, and quantitative computed tomography. DXA is realized as the reference technique to measure BMD in the lumbar spine, proximal femur, forearm, and whole body (2–4).

The World Health Organization (WHO) considers DXA to be the best densitometric technique for assessing BMD. DXA allows accurate diagnosis of osteoporosis, helps to determine the estimate fracture risk and monitoring of patients undergoing treatment (1–5). The primary target of DXA is to quantify BMD accurately and reproducibly and to compare that measurement with a reference population of asymptomatic individuals. Low measurement values on DXA predict the risk of fractures of the spine and hip, analogous to the relationship between high serum cholesterol and the risk of heart disease, or between high blood pressure and the risk of stroke. DXA is also useful in evaluating the effectiveness of FDA-approved therapies for osteoporosis, such as alendronate, risedronate, and raloxifene (1, 2, 4–6).

Positive features of DXA include the safety of its performance, the short investigation time and the ease of use. A DXA measurement may take several minutes to complete with minimal radiation exposure. The densitometer produces ionizing radiation in the form of X-rays and uses laser radiation to position scans. However, the radiation exposure is so low that no shielding of rooms or health professionals is required. The radiation from a DXA scan is less than one would receive during a round trip cross-country airplane flight or during a day of normal background radiation (4, 7, 8).

In measuring BMD, DXA provides a high degree of accuracy, although precision of DXA varies across operators and equipment. Many factors related to the equipment, the operator and the patient determine DXA precision. Operator-related factors are known to contribute to both long- and short-term precision errors. Differences in patient positioning and defining the regions of interest (ROI), both heavily operator dependent, contribute to these variations (3, 7–9). It is estimated that more than five thousand DXA instruments are in regular use worldwide and it is well known that the operators have had widely varied instruction and experience. Operator training in different centers and countries is not standardized, and a lack of knowledge and skill can introduce errors in acquisition, analysis and interpretation of the scans (6, 7, 10).

Common errors in BMD testing can be separated into four categories: 1) indication errors, 2) lack of quality control and calibration, 3) analysis and interpretation errors, and 4) acquisition errors (8–15). Acquisition errors have been well defined in previous studies including improper patient positioning, inappropriate scan mode, invalid skeletal site, persistent artifacts from the scanned area and incorrect demographic information (8–15). To our knowledge, there is no multicenter study that identifies and quantifies acquisition errors in DXA scanning in Turkey.

The aim of this retrospective descriptive multicenter survey is to identify common errors in the acquisition of DXA scanning in Turkey.

Materials and Methods

This descriptive study was conducted retrospectively over a period of 6 months from January 2014 to June 2014, in widely dispersed regions of Turkey. Data analysis and the study were approved by both the local scientific and ethical committees. We analyzed DXA scan results of 20 different centers in 15 different cities in Turkey (Figure 1). The project was approved by the Necmettin University Human Research Ethics Committee (NEUHREC) (Approval number: 2014/662) Individual ethics approval was also obtained from the (NEUHREC) responsible for each of the centers that participated in the project.

Consecutively performed DXA scan results were included the study if each contained a measurement of the lumbar spine and the proximal femur. All available scans performed over the observation period were considered. Forearm measurements, total body measurements or measurements carried out on children were excluded.

Studies were surveyed by 30 consultants from 22 different centers that were informed and trained on DXA scanning principles and standards before the study. Screening was performed according to the following guidelines:

For the lumbar spine (Figure 2a):

- The spine must be centered and straight (centered spinous processes).
- The scan must accurately show L1 through L5, as well as the ribs attached to T12 at the top of the view.

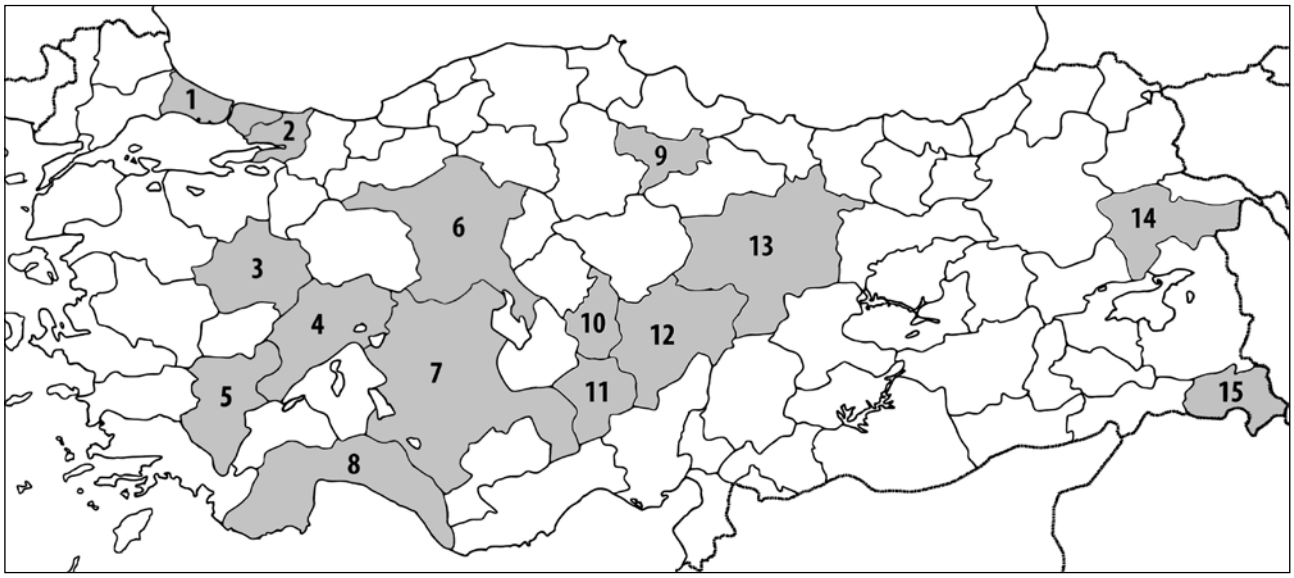

Fig. 1: Locations of DXA sites that contributed to the study: 1. Istanbul, 2. Kocaeli, 3. Kütahya, 4. Afyon, 5. Denizli, 6. Ankara, 7. Konya, 8. Antalya, 9. Amasya, 10. Nevşehir, 11. Niğde, 12. Kayseri, 13. Sivas, 14. Ağrı, 15. Hakkari.

- A small amount of the iliac crest must be visible in the lower corners of the view.
- Similar amounts of soft tissue must appear on each side of the entire spine.
- The region of interest (ROI) must be correctly oriented. ROI areas must include an adequate amount of soft tissue but must not include excessive ribs or iliac crests.
- Marking of vertebrae located in the ROI must be in the correct order.
- ROI must not contain artifacts or foreign bodies like metals, surgical clips, contrast medium, plastic materials, jewelry, body piercings, zippers or buttons.
- The scan must be free of distorting anatomies like laminectomy or spina bifida occulta.
- There must be no conditions that can affect the region being examined or invalidate the measurements like Paget's disease, ankylosing spondylitis, aortic calcification, severe scoliosis or degenerative changes.

For the proximal femur (Figure 2b):

- The image must include the entire femoral head, neck, and approximately 7.5 cm (3 inches) of the femoral shaft.
- The femoral shaft must be aligned parallel to the long dimension of the measurement rectangle.
- The correct amount of soft tissue must be visible lateral to the greater trochanter.
- Internal rotation of the hip must be confirmed by little or no visible lesser trochanter.
- The preferred position for the femoral neck ROI differs depending on equipment manufacturers. The selection of the ROI (greater trochanter, proximal femoral neck or femoral head) must be correct.
- There must be no conditions that can affect the region being scanned or invalidate the measurements like fractures, callus formation or bladder stone.

Also, the specifics of the equipment and the department responsible for the DXA scanning for each institution were recorded.

Statistical analysis of data was performed using the computerized software program SPSS version 13 (SPSS, Inc., Chicago, IL, USA). Variables designed as some categorical (true or false) and derived variables (absolute and percent change) for the statistical analysis plan. Descriptive data were presented as mean ± standard deviation. Demographic and clinical characteristics were compared using the chi-square test. Independent samples t test was used for the comparison of the two groups. A "p" value less than 0.05 was considered as statistically significant.

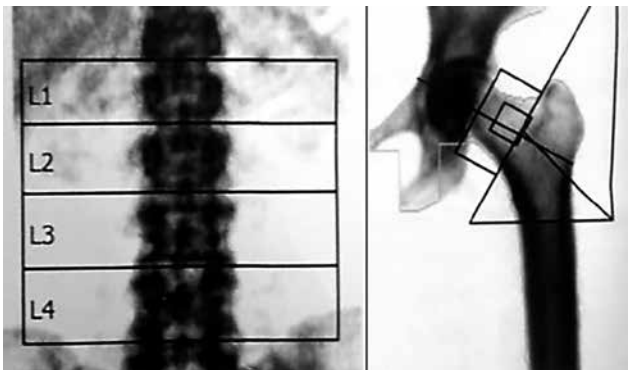

Fig. 2: Correct positioning in lumbar and proximal femur scanning.

Results

A total of 3,212 DXA scan results were examined, acquired from 22 different centers in 15 different Turkish cities. Ten of the 22 centers were state hospitals, 8 were university hospitals, and 4 were training and research hospitals. The Radiology department was responsible for DXA scanning in 12 centers, and the Department of Nuclear Medicine was in charge in 10 centers.

According to our criteria, the percentage of unacceptable results ranged from 10.5% to 65.5% (average 31.7%, n = 1021) for measurement of the lumbar spine and from 21.3% to 74.2% (average 49.0%, n = 1576) in the proximal

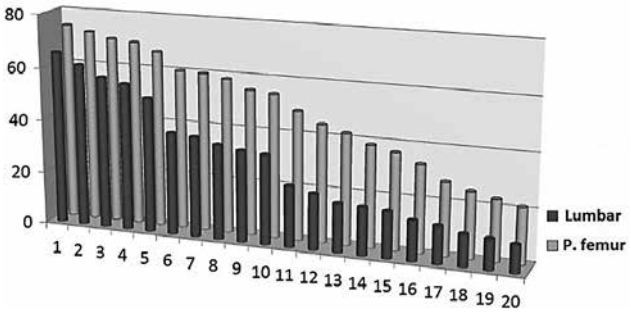

Fig. 3: Error rate in lumbar and proximal femur measurements in each of the 20 centers.

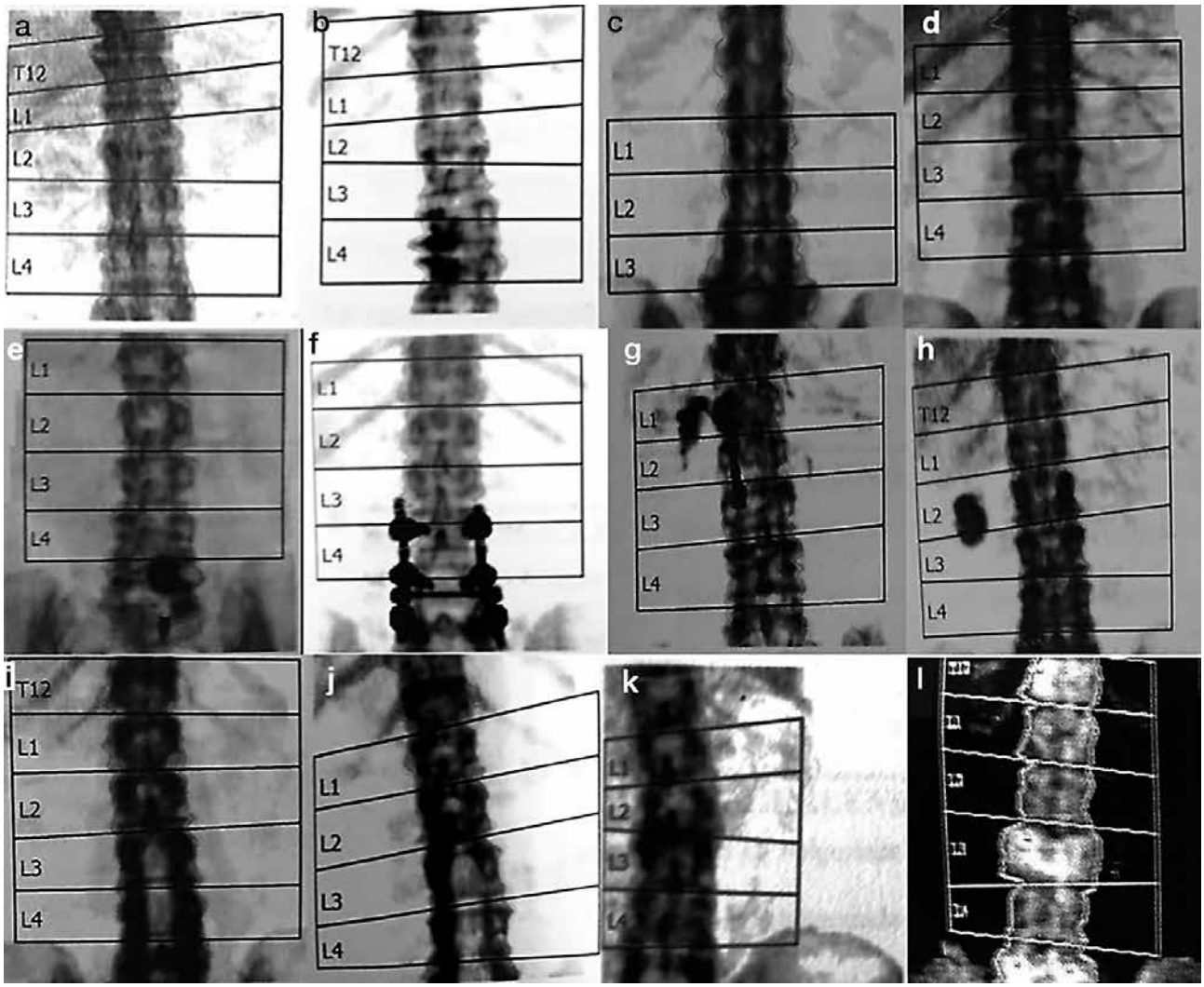

Fig. 4: Common sources of error for lumbar spine DXA measurements.
a/b: Incorrect placing of the ROI (lines should not coincide with the vertebral bodies). **c/d:** Region of interest must be marked in correct order. **e–h:** Artifacts and foreign bodies (**e.** Button and zipper; **f.** Vertebral internal fixator; **g.** Calcification of the omentum and zipper; **h.** Gallstone). **i/j:** Laminectomy defects. **k:** Right-leaning ROI. **l:** Paget's disease.

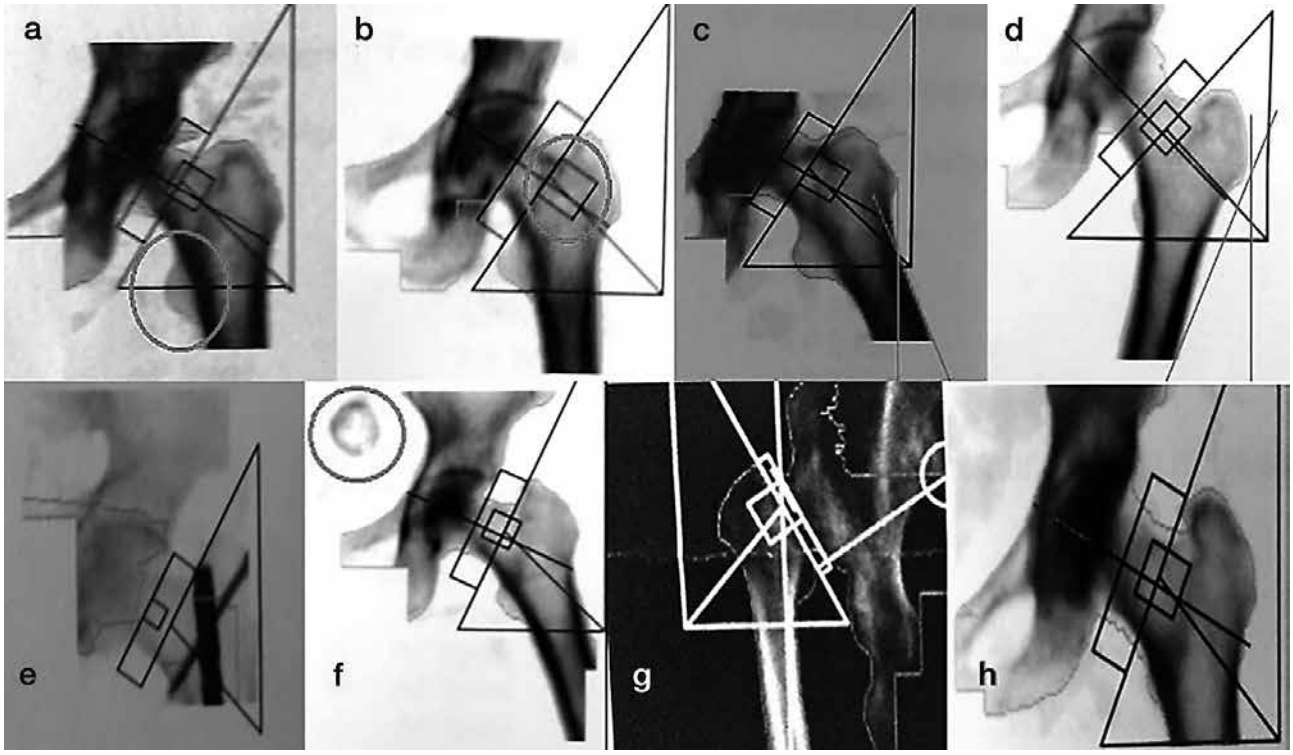

Fig. 5: Common sources of error for proximal femur measurements.
a: Inadequate internal rotation of hip (too much of the lesser trochanter is showing [circle]). **b:** Incorrect femoral neck region of interest placement (region of interest must be set on proximal femur neck). **c:** Exaggerated abduction of the hip. **d:** Exaggerated adduction of the hip. **e–f:** Artifacts or foreign bodies (**e.** Internal fixator in the proximal femur; **f:** Bladder calculus [circle]). **g:** Congenital hip dislocation. **h:** Inappropriately restricted and narrow scan area.

femur (Figure 3). Errors in defining the ROI was the most common error in lumbar spine results (16.2%, n = 522). Other disqualifying problems included the presence of artifacts and foreign bodies, lateral misalignment of the ROI, laminectomy defects, Paget's disease, severe scoliosis and degenerative changes (Figure 4).

Inadequate internal rotation of hip was the most common disqualifying error in proximal femur measurements. Other errors included the faulty definition of the ROI, exaggerated adduction or abduction of the hip, artifacts or foreign bodies in the scanned area, congenital hip dislocation, and restricted or narrow scan area (Figure 5).

There were no statistically significant differences in errors between the state hospitals, the university hospitals or the training and research hospitals ($p > 0.05$). There also were no statistically significant differences between the radiology and the nuclear medicine departments responsible for the measurements ($p > 0.05$).

Discussion

The results of this study show seriously high error rates in DXA assessment of the lumbar spine (31.7%) and the proximal femur (49.0%) in 22 centers in Turkey. Different types of acquisition errors detected in both the lumbar and proximal femur DXA scans were responsible for the mistakes. Data were collected from three classes of hospitals, state, university, and training and research hospitals between which there were no significant differences.

DXA is a clinically proven technique of measuring BMD in the lumbar spine, proximal femur, forearm, and whole body. With DXA, it is possible to measure BMD accurately and reproducibly and to compare that measurement to a reference population of asymptomatic individuals (1–3). Therefore, in the diagnosis and management of osteoporosis and in determining future fracture risk, DXA is the most frequently used method. Some of the challenges in performing reliable DXA measurements include differences in equipment, acquisition techniques, reference databases, reporting methods, and descriptive terminology (7, 8, 10). Much of the responsibility of DXA fall to the operator such as reviewing the patient's skeletal health history, entering demographic data into the computer, performing the image acquisition, and analyzing the scan (8, 10, 13). The operator must evaluate and, if necessary, adjust the computer-selected bone edges and markers of bone ROI. Also, hip bone edges and ROI must be correct, with particular attention paid to the location of the femoral neck box (7–11, 13, 16). Therefore,

DXA clearly is an operator-dependent method. This situation marks the crucial need for education and experience to perform high-quality DXA.

The International Society for Clinical Densitometry (ISCD) is a society with a mission to 1) enhance knowledge, skill, and quality of densitometry among healthcare professionals, 2) educate and certify clinicians and technologists, 3) increase patient awareness, 4) improve access to densitometry, 5) support clinical and scientific advances in the field, and 6) foster the exchange of scientific information. To address these issues, the ISCD periodically holds Position Development Conferences (1, 5, 9). Many guidelines and studies have drawn attention to frequent errors in the clinical use of DXA. Also, there are two available Turkish DXA guidelines (17, 18). However, to our knowledge, no detailed quality assessment and error flagging study of DXA bone mineral density measurement has been carried out across this country. The present study is the first one.

The selection of the ROI can be a major source of error even for experienced operators, especially in roto-scoliosis of the lumbar spine (7, 16, 19). In a typical DXA evaluation, there is usually a gradual increase in vertebral area progressing from L2 to L4. If this is not evident in the results, it is necessary to check the selection of ROI levels (7, 16, 19). In our study, ROI definition errors were the most common problem in lumbar spine measurements (Figure 4a–d).

Kendler et al.(14) used undissolved calcium (Ca) as an artifact to detect the effect on DXA results. They placed the Ca tablets in the soft tissue field, overlying bone and overlapping both bone and soft tissue. An overlying Ca tablet had a considerable effect on BMD, resulting in 12.6% increase in the density of a single vertebral body (14). The Ca tablet artifact showcases the importance of other spine DXA artifacts on imprecision (14). Lumbar spine osteophytes explained 22% of the variation in spine BMD in men and 17% in women. Artifacts such as mal-positioning, osteophytes, and aortic calcification, which could affect BMD, could be seen in the Ca tablet trials (1, 17, 20). In our study, we encountered different types of artifacts such as buttons, zippers, gallstones or nonspecific omental calcification (Figure 4e–h). Abnormal densities are obtained in Paget's disease because of the larger and denser vertebrae. An overlying calcified aorta may raise apparent vertebral density. In addition, absent bony structures, as in laminectomy or spina bifida, or displaced bone as in vertebral rotation due to idiopathic scoliosis could decrease the BMD estimation.

The BMD response following anti-resorptive or anabolic therapy is greater in the lumbar spine than in the proximal femur. However, this progress could be obscured in the presence of degenerative skeletal conditions or by the internal fixation of the lumbar spine. Correct positioning of the patient during the measurement of proximal femur BMD is also vital to obtaining precise values (15, 21). According to cadaveric studies, the minimum BMD in the femoral neck was recorded when the femoral neck was parallel to the examination surface, and gradual increase in BMD occurred when the femur was rotated either internally or externally (22, 23). Therefore, accurate estimation of BMD requires that the axis of the femoral neck be maintained parallel to the inspection surface and perpendicular to the X-ray beam. DXA equipment manufacturers provide different types of positioning aids to achieve this objective. Girard et al. (22) found a significant change in femoral neck BMD when the leg was rotated 10–15° from its neutral position. But Lekamwasam S. et al. (21) examined the effect of leg rotation by 10 degrees either internally or externally on hip BMD in living subjects and concluded that their results show the effect of mal-positioning of the hip during DXA scanning were more significant in longitudinal than in cross-sectional BMD analysis (21). According to our results, inadequate internal rotation of hip was the most common error in proximal femur results. Definition errors of the ROI, excessive adduction or abduction of the hip, artifacts, foreign bodies, congenital hip dislocation, and inappropriate scan area were the other sources of error (Figure 5).

DXA estimates of BMD have been in use for over 20 years in Turkey, and examination protocols continue to improve results (17). There is no educational standard for operator training, and a significant lack of knowledge can lead to flaws in an acquisition, analysis, and interpretation of the scan. Clinical and technical awareness of potential sources of error and artifact are pivotal to maximize the value of DXA measurements of BMD.

Limitations of study

The existing data was gleaned from records of 22 center from 15 provinces of Turkey. Turkey has 81 provinces, and our results that obtained from this study could not generalize to the generalize to the whole country. Although precision errors for DXA scanning evaluated for this study, we don't know the full effects of these errors to the results and how these incorrect measurements effects on the clinical decisions. But this retrospective study helps to focus the question of "frequencies and definitions of common mistakes in the DXA for Turkey" and determines an appropriate sample size. A particularly useful application of this retrospective study is a pilot study that should be completed in anticipation of a prospective trial.

Acknowledgements

Only personal funds were used for this study. No external funds were obtained. Financial disclosure statements have been achieved, and no conflicts of interest have been reported by the authors.

References

1. Sindel D, Gula G. Assessment of Bone Mineral Density in Osteoporosis. Türk Osteoporoz Dergisi 2015; 21: 23–9.
2. Tunç G, Doğan SC, Hizmetli S, Hayta E. In urban areas of Sivas city the determination of bone mineral density reference values of healthy women who admitted to

Cumhuriyet University Hospital Physical Medicine and Rehabilitation outpatient clinic. Türk Osteoporoz Dergisi 2014; 20: 104–9.
3. Sindel D. Osteoporozda görüntüleme yöntemlerinde gelişmeler. Türkiye Klinikleri Journal of Physical Medicine Rehabilitation Special Topics 2009; 2(1): 50–61.
4. Aslan A, Uysal E, Karakoyun Ö. Bone Mineral Density Value in Kastamonu and Area of Turkish Society Women J Clin Anal Med 2013; 4(3): 209–12.
5. Guglielmi G, Ferrari F, Bazzocchi A. Bone Mineral Density and Quantitative Imaging. In: W. C. G. Peh ed. Pitfalls in Diagnostic Radiology. Springer, 2015: 109–32.
6. Allin S, Munce S, Carlin L, Butt D, Tu K, Hawker G, et al. Fracture risk assessment after BMD examination: whose job is it, anyway? Osteoporosis International 2014; 25(5): 1445–53.
7. Lewiecki EM, Lane NE. Common mistakes in the clinical use of bone mineral density testing. Nature clinical practice Rheumatology 2008; 4(12): 667–74.
8. El Maghraoui A, Roux C. DXA scanning in clinical practice. QJM: monthly journal of the Association of Physicians 2008; 101(8): 605–17.
9. Guglielmi G, Diano D, Ponti F, Bazzocchi A. Quality assurance in bone densitometry. Current Radiology Reports 2014; 2(2): 1–6.
10. Khan AA, Colquhoun A, Hanley DA, Jankowski LG, Josse RG, Kendler DL, et al. Standards and guidelines for technologists performing central dual-energy X-ray absorptiometry. Journal of clinical densitometry: the official journal of the International Society for Clinical Densitometry 2007; 10(2): 189–95.
11. Messina C, Bandirali M, Sconfienza LM, D'Alonzo NK, Di Leo G, Papini GD, et al. Prevalence and type of errors in dual-energy x-ray absorptiometry. European radiology 2015; 25(5): 1504–11.
12. Ott SM, Ichikawa LE, LaCroix AZ, Scholes D. Navel jewelry artifacts and intravertebral variation in spine bone densitometry in adolescents and young women. Journal of clinical densitometry: the official journal of the International Society for Clinical Densitometry 2009; 12(1): 84–8.
13. Lewiecki EM, Binkley N, Petak SM. DXA quality matters. Journal of clinical densitometry: the official journal of the International Society for Clinical Densitometry 2006; 9(4): 388–92.
14. Kendler DL, Kiebzak GM, Ambrose CG, Dinu C, Robertson S, Schmeer P, et al. Effect of calcium tablets on interpretation of lumbar spine DXA scans. Journal of clinical densitometry: the official journal of the International Society for Clinical Densitometry 2006; 9(1): 97–104.
15. Wong JCH, Ong B. Evaluation of Femur Angle Abduction/Adduction and Bone Mineral Density Values. Journal of Clinical Densitometry 2005; 8(4): 472–5.
16. Vasić J, Gojković F, Zvekić-Svorcan J, Ćulafić-Vojinović V, Elez J, Filipović K. The most common mistakes in bone mineral density testing with DXA method. MD-Medical data 2013; 5(3): 271–8.
17. Manisali M, Ozaksoy D, Dogan S. Osteoporozda Radyolojik Görüntüleme. Turkiye Klinikleri Journal of Orthopaedics and Traumatology Special Topics 2010; 3(2): 29–38.
18. Erselcan T, Ozen A, Yuksel D, Altun D, Ozturk E, Balci TA, et al. Kemik mineral yoğunluğu ölçümü uygulama kılavuzu. Turk J Nucl Med 2009; 18(1): 31–40.
19. Krueger D, Vallarta-Ast N, Libber J, Checovich M, Gangnon R, Binkley N. Positioner and clothing artifact can affect one-third radius bone mineral density measurement. Journal of clinical densitometry: the official journal of the International Society for Clinical Densitometry 2013; 16(2): 154–9.
20. Richmond B. DXAscanning to diagnose osteoporosis: Do you know what the results mean? Cleveland Clinic Journal of Medicine 2003; 20(4): 353–60.
21. Lekamwasam S, Lenora RS. Effect of leg rotation on hip bone mineral density measurements. Journal of clinical densitometry: the official journal of the International Society for Clinical Densitometry 2003; 6(4): 331–6.
22. Girard MS, Sartoris DJ, Moscona AA, Ramos E. Measured femoral density by dual-energy X-ray absorptiometry as a function of rotation. Orthopaedic review 1994; 23(1): 38–40.
23. Cheng XG, Nicholson PH, Boonen S, Brys P, Lowet G, Nijs J, et al. Effects of anteversion on femoral bone mineral density and geometry measured by dual energy X-ray absorptiometry: a cadaver study. Bone 1997; 21(1): 113–7.

Received: 23/05/2016
Accepted: 29/08/2016

ORIGINAL ARTICLE

Fibroblast Growth Factor-1 Suppresses TGF-β-Mediated Myofibroblastic Differentiation of Rat Hepatic Stellate Cells

*Eva Peterová, Lucie Podmolíková, Martina Řezáčová, Alena Mrkvicová**

Department of Medical Biochemistry, Charles University, Faculty of Medicine in Hradec Králové, Hradec Králové, Czech Republic

* Corresponding author: Charles University, Faculty of Medicine in Hradec Králové, Šimkova 870, 500 38 Hradec Králové, Czech Republic; e-mail: mrkvicovaa@lfhk.cuni.cz

Summary: Myofibroblast expansion is a critical event in the pathogenesis of liver fibrosis. The activation of hepatic stellate cells (HSC) to myofibroblast (MFB) results in the enhanced production of extracellular matrix (ECM). In this study, we explored the effect of acidic fibroblast growth factor (FGF-1) treatment on a transforming growth factor (TGF-β1) induced MFB conversion. We used HSC-T6 cell line, which represents well-established model of activated HSC. These cells strongly expressed α-smooth muscle actin (α-SMA) and fibronectin (FN-EDA) after stimulation with TGF-β1, which is a stimulus for MFB differentiation and ECM production. FGF-1 reduced proteins expression to levels comparable with untreated cells. Mild repression of secreted gelatinases was seen in culture media after FGF-1 treatment. The exposure of cells to collagen gel leads to changes in cell morphology and in expression of MFB markers. Lack of α-SMA in cells embedded to collagen gel was detected. When stimulated with TGF-β1, the cells increased expression of FN-EDA, but not α-SMA. Although the cells on plastic and in collagen gel show different properties, FGF-1 reduced expression of FN-EDA in both conditions. Disrupting TGF-β1 signalling pathway represents a potential strategy for the treatment of fibrosis. We showed that FGF-1 could antagonize signals initiated by TGF-β1.

Keywords: *Myofibroblast; Hepatic stellate cells; Collagen type I; TGF-β1; FGF-1; α -SMA*

Introduction

Hepatic fibrosis is characterized by the excessive deposition of extracellular matrix (ECM). Liver fibrosis was considered to be an irreversible process in the past. Currently it is regarded as a dynamic process arising due to a failure of the normal wound healing. Hepatic stellate cells (HSC), major effector cells, can be activated by many inflammatory cytokines and undergo a myofibroblastic differentiation. Activated HSC are called myofibroblast, because they express high levels of α-smooth muscle actin (α-SMA) and display the ability to contract ECM. While quiescent HSC cells do not synthetize any ECM proteins (3, 13), the activation of MFB results in the enhanced production of ECM components, including collagen types I, III, IV, V, and VI, and fibronectin. This is established as the central event in the development of hepatic fibrosis.

Activated HSC produce wide spectrum of cytokines and respond to their presence via autocrine loop. Transforming growth factor β1 (TGF-β1) is a potent fibrotic factor responsible for the synthesis of the extracellular matrix. TGF-β1 induces the α-SMA expression in fibroblastic cells of various origins (21, 29, 31). TGF-β1 acts through the TGF-β type I and type II receptors to activate intracellular mediators, such as Smad proteins, the p38 mitogen-activated protein kinase (MAPK), and the extracellular signal-regulated kinase pathway (7, 12). Related to this signalling pathway are also fibroblast growth factors (FGFs). FGFs consist of seven families. Basic fibroblast growth factor (FGF-2) and acidic fibroblast growth factor (FGF-1) were found to be widely expressed in tissues. FGFs act through four types of tyrosine kinases receptors (FGFR). A unique feature shared by all members of the FGF family is their strong affinity for the glycosaminoglycan heparin. Heparin is necessary for biological activity of FGF-1. Despite the name, little is known about the effect of FGF-1 on myofibroblast. Few studies suggest that FGF-1, unlike FGF-2, displays antifibrotic functions. FGF-1 has been found to downregulate collagen expression and antagonize profibrogenic effects of TGF-β1. FGF-1 inhibits TGF-β1 induced Smad2 phosphorylation (24, 27), but the mechanism has not been fully elucidated. Our previous study showed that FGF-1 alone decreases the expression of α-SMA and increases the expression of fibronectin (EDA-FN) in fully activated myofibroblasts isolated from a healthy rat liver (22).

Present work aims to elucidate, whether FGF-1 treatment could result in a deactivation of myofibroblasts. Most of studies dealing with MFB have been conducted in the conventional monolayer culture. Three-dimensional collagen matrices are often used as a model to study cell behaviour

ACTA MEDICA (Hradec Králové) 2016; 59(4):124–132
https://doi.org/10.14712/18059694.2017.39

© 2016 Charles University. This is an open-access article distributed under the terms of the Creative Commons Attribution License (http://creativecommons.org/licenses/by/4.0), which permits unrestricted use, distribution, and reproduction in any medium, provided the original author and source are credited.

in the tissue-like environment (9). We provided novel assessment of the effect of FGF-1 on HSC-T6 in collagen gel. The TGF-β1 stimulated HSC-T6 cells (immortalised cells which exhibit the typical features of activated HSC) were treated by FGF-1 and evaluated. Our data indicate that FGF-1 could revert the myofibroblastic differentiation.

To evaluate the effect of FGF-1/H(FGF-1 stabilized with heparin), HSC-T6 cells were stimulated with TGF-β1 for 24 h, and then treated with FGF-1/H in persisting presence of TGF-β1 for another 24 h. Nontreated cells were used as a control group. We examined mRNA expression using qPCR. To validate these results we performed the Western blot analysis and the detection of cellular localization of corresponding proteins using immunocytochemistry.

Methods

Cell cultivation

HSC-T6, an immortalized rat hepatic stellate cell line (34), was kindly gifted from Prof. Weiskirchen, (Institut für Molekulare Pathobiochemie, RWTH Universitätsklinikum Aachen, Germany). HSC-T6 cell line has been known have all features of activated HSC (30). HSC-T6 were cultured in Dulbecco's modified Eagle medium (DMEM, Sigma-Aldrich, Prague, Czechia) containing 10% fetal bovine serum (FBS) (PAA, Cölbe, Germany), 4 mM L-glutamine, 100 U/mL penicillin (Sigma-Aldrich). Cells were maintained at 37 °C in 5% CO_2. After incubation for 24 h in complete DMEM cells were stimulated in serum free medium (SFM) with TGF-β1 (1 ng/ml) for 24 h. To evaluate effect of FGF-1 cells were treated with FGF-1 (4 ng/ml) stabilized with heparin (10 ug/ml) (FGF-1/H) alone or with TGF-β1 (1 ng/ml) for 24 h. Control cells were maintained in SFM. FGF-1 and TGF-β1 were obtained from Peprotech (Rocky Hill, USA), heparin from porcine intestinal mucosa was obtained from Sigma-Aldrich.

Collagen gel

Rat tail collagen type I was prepared as described in Peterova et al. 2016. The cells (60 thousands) were suspended in 2 ml of mixture of sterile collagen solution with 4 × DMEM in the ratio 3:1 (v/v). The gels were allowed to polymerize in the CO_2 incubator for 1 hour at 37 °C in Petri 35 mm dishes. First layer was covered with the same volume of DMEM containing 20% FBS and antibiotics. After incubation for 24 h in complete DMEM cells were stimulated in serum free medium (SFM) with TGF-β1 and FGF-1/H as described elsewhere.

RNA isolation and quantitative reverse transcription polymerase chain reaction (qRT-PCR)

The cells on plastic were washed with phosphate-buffered saline (PBS), harvested and dissolved in RLT lysis buffer (Qiagen, RNeasy Mini kit). Total cellular RNA was extracted by RNeasy Mini kit according to manufacturer instructions (Qiagen, Hilde, Germany). Collagen gel was dissolved by Clostridium histolyticum collagenase NB 4G proved grade (Serva, Heidelberg, Germany). 1 ug of RNA was reverse transcribed using cDNA Reverse Transcription Kit and quantified with TaqMan Gene Expression Assays (TGF β1 Rn00572010_m1, Acta1 Rn01426628_g1, Fndc3a Rn01465936_m1, Col1a2 Rn00584426_m1, MMP2 Rn01538171_m1, TIMP1 Rn00587558_m1) using 7500 Fast Real-Time PCR system (all obtained from Applied Biosystems, Prague, Czechia). The relative expression from four independent experiments performed in duplicates was normalized to 18 s expression.

Western blot analysis

The cells were harvested, suspended in PBS containing 4 mM EDTA and washed 3 times. Collagen gels were dissolved. The proteins were extracted with Cell lysis buffer 10× (Cell Signaling Technology, Danvers, USA). Protein content was determined by Bicinchoninic Acid Protein Assay Kit (Sigma-Aldrich). Forty μg of protein were applied on Novex NuPAGE 4–12% Bis-Tris gel (Invitrogen Life Technologies, Prague, Czechia) under nonreducing conditions. The proteins were transferred to 0.2 μm Hybond nitrocellulose membrane (GE Healthcare, München, Germany). Staining with Ponceau S was used as a loading control. The membranes were incubated with antibodies to α-SMA (1A4, Sigma-Aldrich), cellular fibronectin (IST-9, Santa Cruz Biotechnology, Santa Cruz, USA) or MMP-2 (H-76, Santa Cruz), TIMP-1 (Santa Cruz) at 4 °C overnight. The secondary antibodies were from Santa Cruz. Detection was done with Western Blotting Luminol Reagent (Santa Cruz). The blots were scanned, quantified by program QUANTITY ONE 4.6 (Bio-Rad Laboratories, Hercules, California) and normalized to the respective controls.

Immunocytochemistry

The cells were fixed in 98% ethanol for 10 minutes. They were permeabilized on ice in cold solution of 0.1% Triton X-100 in 0.1% sodium citrate for 5 min. Nonspecific binding sites were blocked by 10% fetal calf serum in PBS for 30 min. The cells were incubated with the primary antibody at 4 °C overnight. Anti-α-smooth muscle actin (α-SMA) clone 1A4 (Sigma-Aldrich) was diluted 1:400. The secondary antibody was Polyclonal Goat Anti-mouse immunoglobulins/HRP (Dako, Glostrup, Denmark); it was diluted 1:100 and the cells were incubated in the dark for 1 hour. Nuclei were stained with 4′,6-diamidino-2-phenylindole (DAPI, Sigma-Aldrich) for 2 min. Unspecific mouse immunoglobulins served as negative controls. Cells were washed with PBS, mounted in Vectashield (Vector Laboratories, Burlingame, California) and studied under Nikon Eclipse fluorescent microscope.

Gelatin zymography

Zymographic analysis was performed on conditioned media. The cells cultured on gels were released with trypsin and plated on plastic for 24 hours. The medium was collected and compared with the medium of trypsinized cells cultured previously on plastic only. Protein concentration in the media was adjusted to 1 mg/ml. Ten microliter aliquots were electrophoresed in 8% SDS-polyacrylamide gel containing 0.1% gelatin (Sigma-Aldrich). The gel was washed in 2.5% Triton X-100 for 1 h and subsequently incubated for 15 h at 37 °C in 50 mmol/L Tris-HCl buffer pH 7.4 containing 15 mmol/L sodium chloride and 10 mmol/L calcium chloride. The gel was stained with Coomasie brillant blue and destained with 40% methanol and 10% acetic acid solution. Gelatinolytic bands were size-calibrated with a high molecular mass marker (Bio-Rad).

Statistical analysis

Results are presented as mean ± SD. Statistical significance of differences between groups was tested with one-way ANOVA. Significant results are shown wit asterisk (* $P \leq 0.05$; ** $P \leq 0.01$). All calculations were performed using GraphPad Prism version 6.00 for Windows, GraphPad Software (San Diego, California USA).

Results

TGF-β1-induced myofibroblastic conversion is reversed by FGF-1/H

Figure 1 shows that stimulation of HSC-T6 with TGF-β1 resulted in an increased mRNA expression of myofibroblast markers TGF-β1 (3 fold) and α-SMA (135 fold), but not that of fibronectin. Non-significant increase in an expression of collagen type I gene COL1A2 was observed. The addition of FGF-1/H decreased the mRNA expression of TGF-β1 to similar levels that were observed in unstimulated cells. No effect of FGF-1/H on mRNA expression of fibronectin or COL1A2 was observed (Fig. 1A). On the protein level, however, α-SMA and fibronectin protein amounts were changed during the treatment, as confirmed by Western blot and immunohistochemical analysis. Compared with TGF-β1 treated cells, the addition of FGF-1/H led to a drastic decrease of fibronectin and α-SMA protein levels, indicating a positive effect on the antimyofibroblastic conversion (Fig. 1B). Reduced α-SMA expression after the FGF-1/H treatment (as visualized by immunofluorescence) supported these results. Upon stimulation or FGF1/H treatment the cells did not exhibit any morphological changes; proliferation was also unaffected (data not shown).

Protective effect of collagen gel on FGF-1/H-induced reversal of myofibroblastic activation

The importance of collagen environment on cell behaviour, phenotype and proliferation is widely accepted (10). Cytokine induced myofibroblastic conversion and its reversal should be therefore confirmed under condition which could mimic in vivo fibrotic condition.

Figure 2 shows the effect of collagen gel cultivation on the expression of myofibroblastic markers during TGF-β1 stimulation and FGF-1/H treatment. Cells were planted into the collagen type I gel. Collagen type I is almost not present in the space of Disse in a healthy liver. It becomes abundant during liver fibrosis progress due to HSC proliferation, activation and myofibroblastic conversion. When grown in collagen gel, HSC-T6 cell tend to clump together. Protrusions radiating from the outer margin of the clump are frequent (Fig. 2C). The cells in collagen gel responded to TGF-β1 stimulus by an enhanced mRNA expression of α-SMA (3fold). Addition of TGF-β1 did not paracrinally stimulate TGF-β1 gene expression, as seen on plastic. Also, no induction of COL1A2 or fibronectin genes was observed (Fig. 2A). Despite of the enhanced α-SMA mRNA expression, we could not detect any changes at a protein level. More interesting is the fact that a control group of cells growing in the collagen gel had highly reduced levels of α-SMA (non-detectable using immunofluorescence, Fig. 2C) compared to cells grown on plastic. FN-EDA was the only one of the tested markers that behaved in the same way in the cells cultivated on the plastic and in the collagen gel. An upregulation of FN-EDA protein expression after the TGF-β1 treatment was detected; addition of FGF-1/H reduced it.

FGF-1/H effect on the proteolytic phenotype of HSC-T6 on the plastic

ECM remodelling is mostly carried out by the balance between activities of proteinases and their inhibitors. We tested cytokine mediated regulation of gelatinases MMP-2, MMP-9 and tissue inhibitors of MMP (TIMP-1, TIMP-2) on different substrates. Figure 3 shows the effect of TGF-β1 cell stimulation and FGF-1/H treatment on amount of mRNA of MMP-2, MMP-9, TIMP-1, and TIMP-2 (Fig. 3A). Protein expressions of MMP-2 and TIMP-1 are also shown (Fig. 3B). TGF-β1 stimulated the mRNA expressions of MMP-2, MMP-9 and TIMP-1 in HSC-T6. FGF-1/H attenuated the expression of TIMP-1 to levels comparable to those expressed by the untreated cells. Western blot showed that MMP-2 and TIMP-1 protein expression did not parallel the changes observed at the mRNA level. Neither the amount of the full-length 72 kDa pro-MMP-2, nor the amount of fully active MMP-2 62 kDa form was changed after the TGF-β1 cell stimulation or the FGF-1/H treatment. TGF-β1 promotes a TIMP-1 protein expression that remained the same after the FGF-1/H treatment. Finally, enzyme activity of MMP-2 and MMP-9 was measured by the gelatin zymography (Fig. 3C). Sample processing (involving de- and re-naturation) restores active form of the MMP, but also the gives the ability to digest gelatin to the normally inactive pro-MMPs. Gelatinolytic activities corresponding to the latent forms of MMP-2 and MMP-9 were present in conditioned media

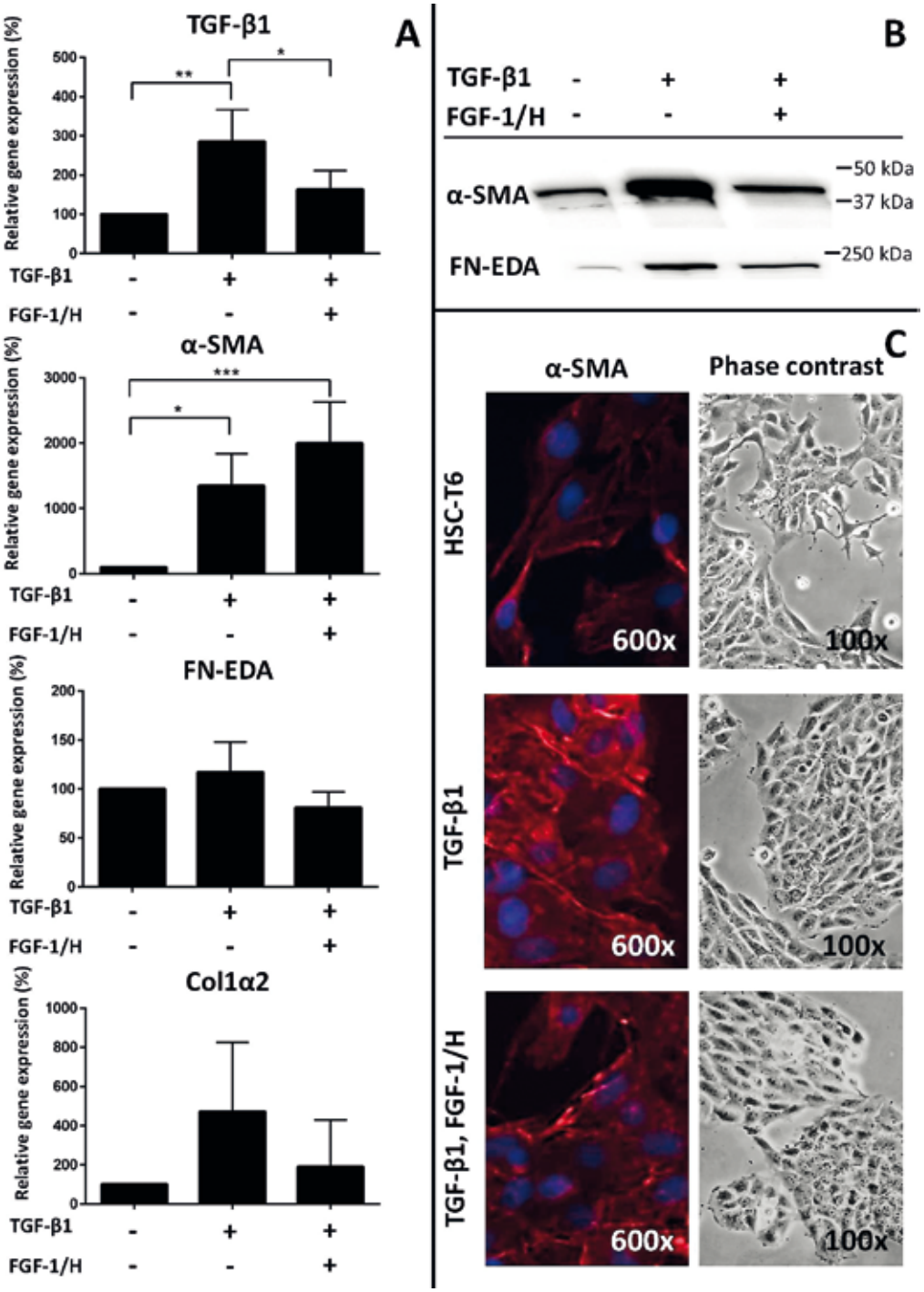

Fig. 1: Effect of FGF-1/H on the expression of myofibroblastic markers. Cells were treated with TGF-β1 for 24 h, then for another 24 h with FGF-1/H in combination with TGF-β1 or TGF-β1 alone. Stimulation of HSC-T6 with TGF-β1 resulted in increased expression of TGF-β1and α-SMA mRNA measured by qRT-PCR. Addition of FGF-1/H attenuated the expression of TGF-β1. COL1A2 and fibronectin expression did not significantly respond to the treatment with FGF-1/H (A). Each bar represents mean ± SD. Western blot for α-SMA and fibronectin revealed increased expression of both proteins after TGF-β1 stimulation., followed by decreased expression after FGF-1/H treatment (B). Four independent experiments were performed, statistical significance * $p \leq 0.05$, ** $p \leq 0.01$. Presence of α-SMA (red) in HSC-T6 cell was detected by immunofluorescence (C). Nuclei were counterstained with DAPI (blue). Magnification (600×). Strong expression of α-SMA was seen in the cells treated with TGF-β1. Immunoreactivity was partially reduced after FGF-1/H treatment. The cells under phase contrast with lower magnification (100×) are also presented (C right panel).

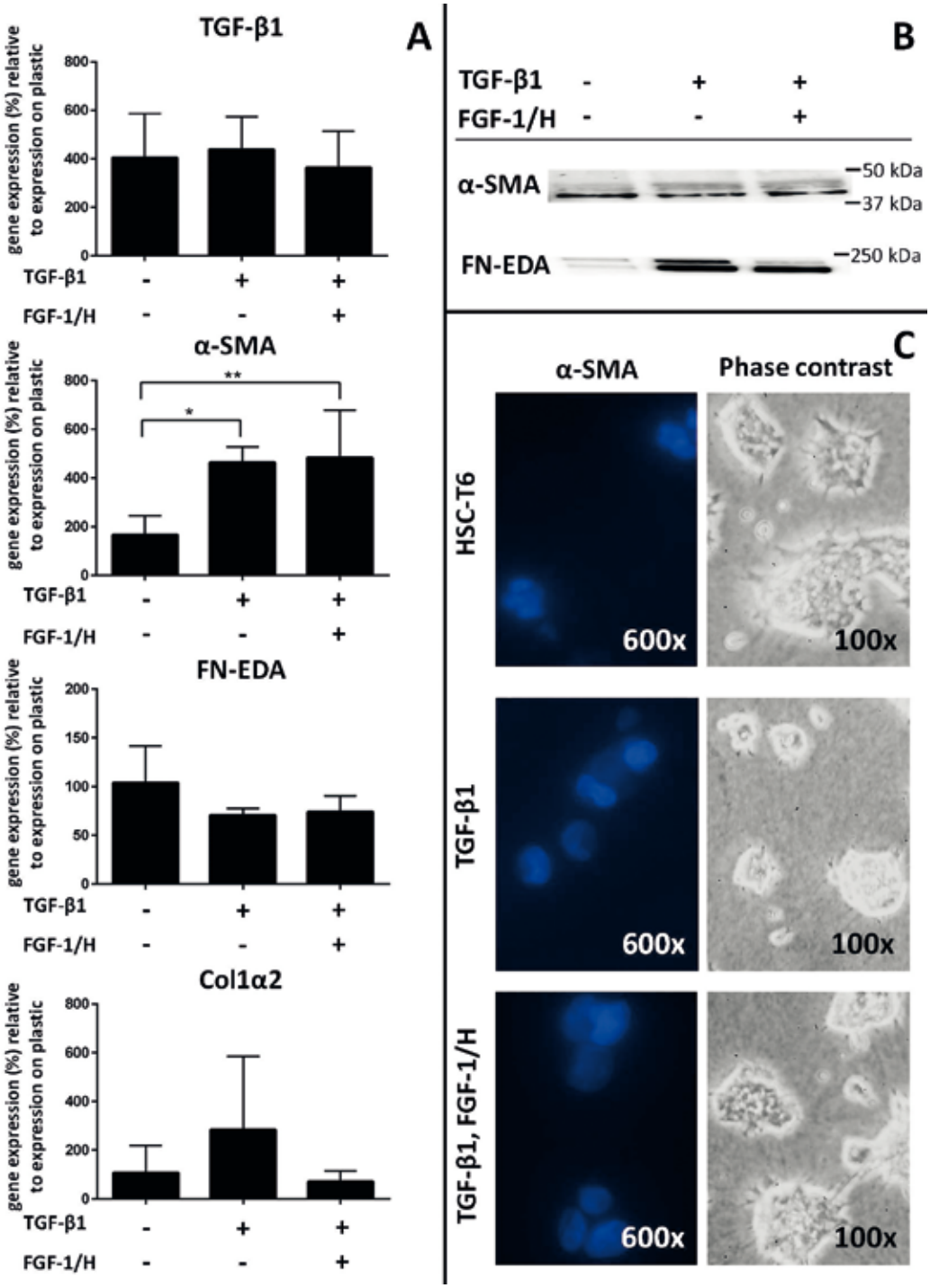

Fig. 2: Effect of collagen gel cultivation on FGF-1/H-induced myofibroblast deactivation. The cells were seeded in the three dimensional collagen gel and treated with TGF-β1 for 24 h, then for another 24 h with FGF-1/H in combination with TGF-β1 or TGF-β1 alone. Expression of markers of myofibroblastic conversion was measured using qRT-PCR Graphs (A) show the changes in mRNA expression levels with or without treatment (cells seeded on plastic dishes are set as 100%). Each bar represents mean ± SD. Four independent experiments were performed, statistical significance * $p \leq 0.05$, ** $p \leq 0.01$. Western blot for α-SMA showed weak positivity in the cells in the collagen gel, no induction by TGF-β1 treatment was seen. Fibronectin appeared after stimulation and the total protein levels drop after FGF-1 treatment (B). Neither unstimulated cells not stimulated or FGF-1 treated cells showed α-SMA positivity as detected by immunofluorescence, only DAPI stained nuclei are visible (C). Cell under phase contrast are shown (C right panel).

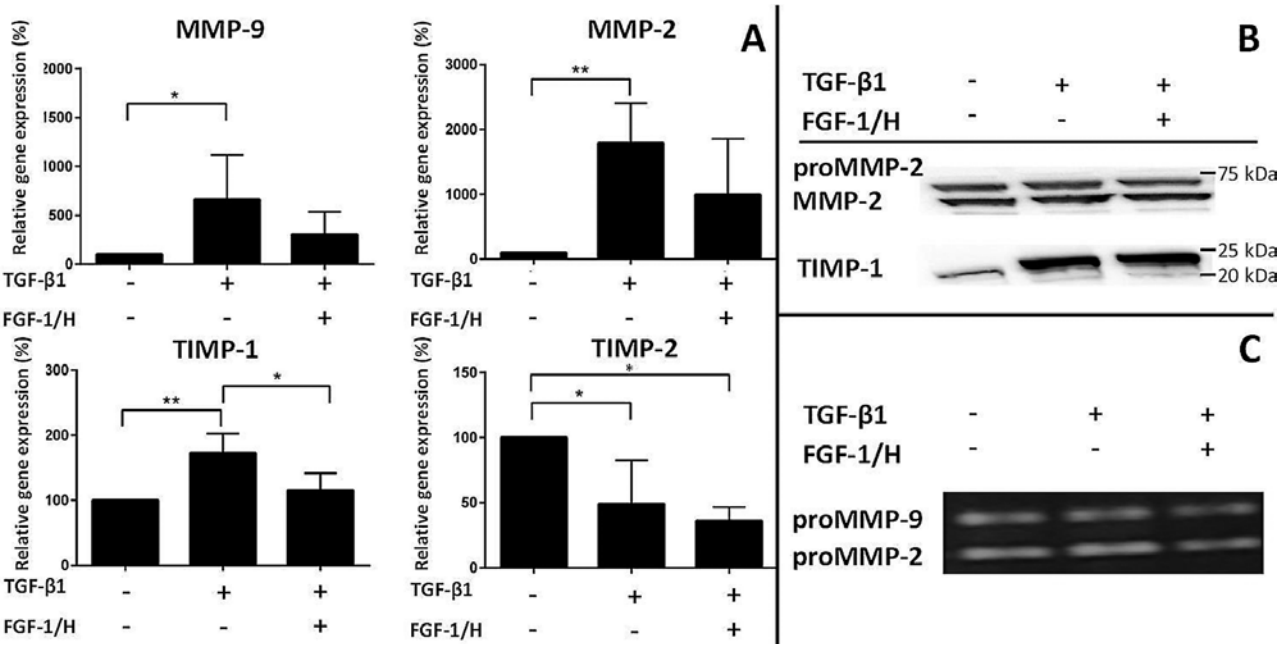

Fig. 3: Effect of FGF-1/H on the expression of gelatinases and MMP inhibitors. The cells were cultivated on plastic and treated with TGF-1 for 24 h, then for another 24 h with FGF-1/H in combination with TGF-β1 or TGF-β1 alone. Stimulation of HSC-T6 with TGF-β1 resulted in the increased expression of MMP-2, MMP-9 and TIMP-1 mRNA measured by qPCR. Addition of FGF-1/H attenuated the expression of MMP-2, MMP-9 and TIMP-1 (A). Each bar represents mean ± SD. Four independent experiments were performed, statistical significance * $p \leq 0.05$, ** $p \leq 0.01$. In contrast, neither the TGF-β1 stimulation nor the FGF-1/H treatment had any significant effect on the MMP-2 expression at a protein level (B). Expression of TIMP-1 protein increased after the TGF-β1stimulation. MMP-2 and MMP-9 activity was detected by a gelatin zymography. The FGF-1/H treatment mildly reduced pro-MMP-2 release into the culture media (C).

of HSC-T6. TGF-β1 slightly induced pro-MMPs secretion, while FGF-1/H repressed it.

FGF-1/H effect on the proteolytic phenotype of HSC-T6 in the collagen gel

HSC-T6 cells were embedded in the collagen gel, followed by the cytokine stimulation. We found different expression patterns of the non-stimulated cells on the plastic and in the collagen gel. Graph 4 shows mRNA expressions of MMP-2, 9, and TIMP-1, 2 indicated as a percentage of the unstimulated control HSC-T6 seeded on plastic. Planting of the cells into the collagen gel alone dramatically increased MMP-2 expression. No effect of TGF-β1 or FGF-1 on mRNA expression of genes of interest was observed. Western blot analysis revealed that TGF-β1 induced expression of pro-MMP-2, however, most of it remained as a zymogen without being converted to the active form. In the collagen gel, the HSC-T6 cells secrete less MMP-2 and 9 in response to FGF-1 treatment.

Discussion

In the presented work, we demonstrate that FGF-1/H prevents TGF-β1-induced myofibroblastic activation, as evidenced by decreased levels of α-SMA and FN-EDA. We also provide the evidence that MFB phenotypic switch is modulated by ECM. This finding is consistent with our previous work showing that FGF-1/H alone had a larger effect on MFB phenotype in the cells cultured on plastic than on those in collagen gel (22). In the previous study, fully activated MFB were generated by outgrowth of primary HSC, isolated from a normal rat liver. MFB and HSC differ in the ability to degrade ECM proteins. MFB represent a cell population with high collagenolytic potential (15), which HSC-T6 do not have. Thus the HSC-T6 cells can reflect an early phase of the liver damage, when cytokines play a crucial role in the activation of quiescent HSC.

The key cells participating in the development of the liver fibrosis are HSC and MFB. In the intact liver, HSC store retinoids and triacylglycerols in cytoplasmic lipid droplets. After a liver injury, HSC are activated into contractile MFB. Cytokines released from damaged hepatocytes and Kupfer cells are major stimulants (26). TGF-β1 appears to be responsible for the stimulation of ECM proteins expression and inhibition of their degradation (4, 8). An important property of TGF-β1 is the ability to induce its own mRNA expression, and thereby multiply its effect (32). TGF-β1 induces mRNA expression of MFB markers, such as α-SMA, procollagen, and fibronectin (17). It was

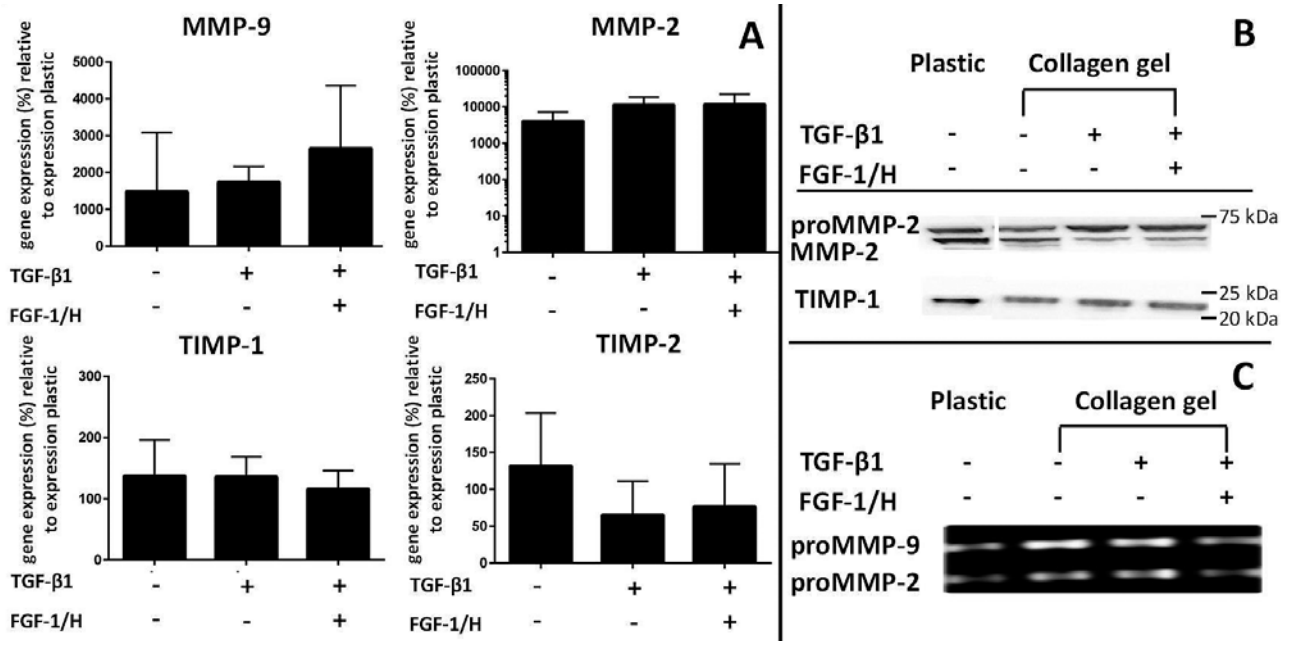

Fig. 4: Effect of FGF-1 on the expression of gelatinases and tissue inhibitors in the collagen gel. The cells were cultivated in the collagen gel, treated with TGF-β1 for 24 h, then for another 24 h with FGF-1/H in combination with TGF-β1 or TGF-β1 alone. TGF-β1 stimulation or FGF-1/H treatment did not t induce any significant changes in mRNA expression (cells seeded on plastic dishes are set as 100%). Each bar represents mean ± SD. Four independent experiments were performed. TGF-β1 induced expression of pro-MMP-2, but not of the active form (B). Gelatinase activity was measured by a gelatin zymography (C).

proved by others (6) that the α-SMA and FN positive cells are responsible for the overproduction of collagen type I in a fibrotic liver. Moreover, there is a correlation between expressions both proteins. Cellular FN consists of two splicing variants, namely ED-A and ED-B. It was shown that TGF-β1 increases accumulation of the ED-A FN isoform (1). TGF-β1 induction of ED-A FN is dependent on PI3-kinase-AKT signalling (23). Our results on HCS-T6 showed that TGF-β1 indeed induced its own mRNA expression and expression of α-SMA, but had no effect on mRNA expression of procollagen I. Increase in fibronectin was detected in the TGF-β1 stimulated cells at the protein level. The effect of FGF-1/H on HSC-T6 was ambiguous. It decreased the TGF-β1 auto-induction, but conversely also potentiated the expression of α-SMA mRNA. More importantly, FGF-1/H reduced α-SMA and fibronectin at protein levels. Our data show that FGF-1 is sufficient to reduce the myofibroblastic differentiation, but the mechanism is not solely based on the downregulation of expression of the related genes. Our findings correspond with previous studies, suggesting that FGF-1 has an antifibrotic role: The myofibroblast phenotype reversal induced by FGF-1/H has been described in lung fibroblasts. Cells treated with FGF-1/H displayed increased apoptosis, decreased collagen production, and α-SMA expression (25). FGF-1 also has the ability to revert EMT by inhibiting Smad2 phosphorylation through the MAPK/ERK pathway (24, 27).

Cells-to-matrix interaction could modify the phenotype of the myofibroblasts. Therefore, an understanding of this cooperation requires the use of the matrix-derived lattices. Various 2D or 3D matrices were studied in order to determine the influence of ECM on the myofibroblast activation. Collagen gels are used to mimic in vivo fibrotic conditions (10). It was published that TGF-β1 stimulates a contraction of native collagen gels by HSC, these properties of HSC associated with an increase in α-SMA content. This contraction was dependent on a HSC cell density in the collagen lattices (16). Others have reported that TGF-β1-induced increase of α-SMA content in a human gingival fibroblasts is dependent on the resistance of the substrate to deformation. Soft environment, represented by floating gels, did not increase mRNA for α-SMA at all (2). The interaction of the collagen gel fibres with α2β1-integrin may be a restriction factor in stretch-induced α-SMA and FN-EDA regulation. In our study we induced the myofibroblastic phenotype on both substrata – plastic dishes, which represent condition with high tensile strength, and the opposite collagen gel lattice, with a low tensile strength. We show that in HSC-T6 cells TGF-β1 fails to induce the α-SMA protein expression in the collagen gel. The TGF-β1 stimulation appears to associate with an increase in FN-EDA. The FGF-1 treatment was able to markedly reduce this expression. We also provided the evidence that the α-SMA expression is accompanied with the FN-EDA increase on the plastic as suggested by others

(14, 33), but not in the collagen gel. Taken together, myofibroblasts are plastic cells that – if stimulated – can express some (but not all) profibrogenic markers. This expression is modulated by the three-dimensional environment. The FGF-1 treatment could possibly diminish some of these changes.

Proteolysis of ECM is a key player in the resolution of a liver fibrosis. The matrix degradation is achieved by the activity of MMPs, which consists of collagenases, gelatinases, stromelysins, and membrane type (MT)-MMPs. Various cytokines and growth factors, including TGF-β1, control the balance between activators and inhibitors of proteinases. During an acute liver injury elevated levels of TGF-β1, MMP-2, MMP-9, and TIMP-1 were found, suggesting their role in the early ECM remodelling (18). MMP-9 was found in scaring areas along with the activated HSC (11). TGF-β1 stimulated expression of MMP-2 and TIMP-1 in vitro in dose dependent manner (19, 20). In our hands, stimulation of the cells with TGF-β1 promoted MMP-2, MMP-9 and TIMP-1 expression and reduced the expression of TIMP-2, but no changes at the protein level were detected.

According to our previous results we presumed that FGF-1 might influence MMP and TIMP expression. A mild repression of secreted pro-MMP-2 and pro-MMP-9 was seen in culture media in the FGF-1/H treated cells. FGF-1/H presence reduced the TIMP-1 mRNA expression significantly. TIMP-1 is important in the inhibition of collagenase (MMP-1) and MMP-9, while TIMP-2 regulates the activity of MMP-2. Increase in the capacity for ECM turnover by reduction of protease inhibition is the goal of an anti-fibrotic therapy. Previous studies showed that 3D environment rich in type I collagen stimulates the ECM remodelling activities of HSC by induction of MMP-9 (18, 28). Collagen gel stimulates mRNA expression of MMP-2 as well as its activity in HSC-T6 cells. Mild decrease in secretion of pro-MMP-2 and pro-MMP-9 in the FGF-1/H treated cells was seen.

Conclusion

To address the effect of FGF-1 on myofibroblastic conversion of HSC-T6 cells, thecells were stimulated with TGF-β1. The cells were cultivated in the monolayer cultures or on the collagen gels. FGF-1 significantly reduced levels of FN-EDA in the both environments, and significantly reduced levels of α-SMA on plastic For this reason we conclude that FGF-1 could (by an unknown mechanism) antagonize the signals initiated by TGF-β1; FGF-1 is thus behaving as an antagonist of induction of myofibroblastic features in both plastic and in three-dimensional collagen matrices. FGF-1 represents a possible agent for pharmacological studies on the myofibroblastic activation during pathological events.

Acknowledgements

This work was supported by the project PRVOUK P37/01 and SVV-2016-260287.

References

1. Adapala RK, Thoppil RJ, Luther DJ, et al. TRPV4 channels mediate cardiac fibroblast differentiation by integrating mechanical and soluble signals. Journal of Molecular and Cellular Cardiology 2013; 54: 45–52.
2. Arora PD, Narani N, McCulloch CAG. The Compliance of Collagen Gels Regulates Transforming Growth Factor-β Induction of α-Smooth Muscle Actin in Fibroblasts. The American Journal of Pathology 1999; 154: 871–882.
3. Bataller R, Brenner DA. Liver fibrosis. Journal of Clinical Investigation 2005; 115: 209–218.
4. Braunersreuther V, Viviani GL, Mach F, Montecucco F. Role of cytokines and chemokines in non-alcoholic fatty liver disease. World Journal of Gastroenterology 2012; 18: 727–35.
5. Broekelmann TJ, Limper AH, Colby TV, McDonald JA. Transforming growth factor beta 1 is present at sites of extracellular matrix gene expression in human pulmonary fibrosis. Proceedings of the National Academy of Sciences of the United States of America 1991; 88: 6642–6646.
6. Carpino G, Morini S, Corradini SG, et al. Alpha-SMA expression in hepatic stellate cells and quantitative analysis of hepatic fibrosis in cirrhosis and in recurrent chronic hepatitis after liver transplantation. Digestive and Liver Disease 2005; 37: 349–356.
7. Derynck R, Muthusamy BP, Saeteurn KY. Signaling pathway cooperation in TGF-β-induced epithelial–mesenchymal transition. Current Opinion in Cell Biology 2014; 31: 56–66.
8. Gressner AM, Weiskirchen R, Breitkopf K, Dooley S. Roles of TGF-beta in hepatic fibrosis. Frontiers Bioscience 2002; 7: 793–807.
9. Grinnell F, Petroll WM. Cell motility and mechanics in three-dimensional collagen matrices. Annual Review of Cell and Developmental Biology 2010; 26: 335–361.
10. Grinnell F. Fibroblast biology in three-dimensional collagen matrices. Trends in Cell Biology 2003; 13: 264–269.
11. Han YP. Matrix metalloproteinases, the pros and cons, in liver fibrosis. Journal of Gastroenterology and Hepatology 2006; 21(suppl 3): S88–S91.
12. Huang C, Day ML, Poronnik P, Pollock CA, Che XM. Inhibition of KCa3. 1 suppresses TGF-β1 induced MCP-1 expression in human proximal tubular cells through Smad3, p38 and ERK1/2 signaling pathways. The International Journal of Biochemistry & Cell Biology 2014; 47: 1–10.
13. Iredale JP, Thompson A, Henderson NC. Extracellular matrix degradation in liver fibrosis: Biochemistry and regulation. Biochimica et Biophysica Acta (BBA) – Molecular Basis of Disease 2013; 1832: 876–83.
14. Jarnagin WR, Rockey DC, Koteliansky VE, Wang SS, Bissell DM. Expression of variant fibronectins in wound healing: cellular source and biological activity of the EIIIA segment in rat hepatic fibrogenesis. The Journal of Cell Biology 1994; 127: 2037–2048.
15. Jiroutova A, Peterova E, Bittnerova L, et al. Collagenolytic potential of rat liver myofibroblasts. Physiological Research 2013; 62: 15–25.
16. Kharbanda KK, Rogers DD, Wyatt TA, Sorrell MF, Tuma DJ. Transforming growth factor-β induces contraction of activated hepatic stellate cells. Journal of Hepatology 2004; 41: 60–66.
17. Kim SJ, Ballock RT. Cellular and molecular biology of Transforming Growth Factors. In: Nosa M. Cellular and Molecular Biology of Bone 2014; 98: 122.
18. Knittel T, Mehde M, Kobold D, Saile B, Dinter C, Ramadori G. Expression patterns of matrix metalloproteinases and their inhibitors in parenchymal and non-parenchymal cells of rat liver: regulation by TNF-α and TGF-β1. Journal of Hepatology 1999; 30:48–60.
19. Kwak HJ, Park MJ, Cho H, et al. Transforming growth factor-β1 induces tissue inhibitor of metalloproteinase-1 expression via activation of extracellular signal-regulated kinase and Sp1 in human fibrosarcoma cells. Molecular Cancer Research 2006; 4: 209–220.
20. Mecha EO, Sui C, Omwandho CO, Tinneberg HR, Konrad L. Transforming Growth Factor Betas induce MMP-2 and MMP-9 Secretion via Smad-dependent Signaling in Human Endometrial and Endometriotic Cells. International Journal of Scientific Engineering and Technology 2015; 4: 567–72.
21. Mun JH, Kim YM, Kim BS, Kim J. H, Kim MB, Ko HC. Simvastatin inhibits transforming growth factor-β1-induced expression of type I collagen, CTGF, and α-SMA in keloid fibroblasts. Wound Repair and Regeneration 2014; 22: 125–33.
22. Peterová E, Mrkvicová A, Podmolíková L, Řezáčová M, Kanta J. The role of cytokines TGF-beta1 and FGF-1 in the expression of characteristic markers of rat liver myofibroblasts cultured in three-dimensional collagen gel. Physiological Research 2016; 65: 661–72.
23. Phanish MK, Heidebrecht F, Nabi ME, Shah, N, Niculescu-Duvaz I, Dockrell MEC. The regulation of TGF-β1 1 induced fibronectin EDA exon alternative splicing in human renal proximal tubule epithelial cells. Journal of Cellular Physiology 2015; 230: 286–295.
24. Ramos C, Becerril C, Montaño M, et al. FGF-1 reverts epithelial-mesenchymal transition induced by TGF-β1 through MAPK/ERK kinase pathway. American Journal of Physiology – Lung Cellular and Molecular Physiology 2010; 299: L222–L231.

25. Ramos C, Montaño M, Becerril C, et al. Acidic fibroblast growth factor decreases α-smooth muscle actin expression and induces apoptosis in human normal lung fibroblasts. American Journal of Physiology – Lung Cellular and Molecular Physiology 2006; 291: L871–L879.
26. Reeves HL, Friedman SL. Activation of hepatic stellate cells – a key issue in liver fibrosis. Frontiers Bioscience 2002; 7: 808–826.
27. Shimbori C, Bellaye PS, Xia J, et al. Fibroblast growth factor-1 attenuates TGF-β1-induced lung fibrosis. The Journal of Pathology 2016; 240: 197–210.
28. Takahara M, Naruse T, Takagi M, Orui H, Ogino, T. Matrix metalloproteinase-9 expression, tartrate-resistant acid phosphatase activity, and DNA fragmentation in vascular and cellular invasion into cartilage preceding primary endochondral ossification in long bones. Journal of Orthopaedic Research 2004; 22: 1050–57.
29. Thakur S, Viswanadhapalli S, Kopp JB, et al. Activation of AMP-Activated Protein Kinase Prevents TGF-β1-Induced Epithelial-Mesenchymal Transition and Myofibroblast Activation. The American Journal of Pathology 2015; 185: 2168–80.
30. Vogel S, Piantedosi R, Frank J, et al. An immortalized rat liver stellate cell line (HSC-T6): a new cell model for the study of retinoid metabolism in vitro. Journal of Lipid Research 2000; 41: 882–893.
31. Wang Y, Lin C, Ren Q, Liu Y, Yang X. Astragaloside effect on TGF-β1, SMAD2/3, and α-SMA expression in the kidney tissues of diabetic KKAy mice. International Journal of Clinical and Experimental Pathology 2015; 8: 6828–34.
32. Wen FQ, Kohyama T, Sköld CM, et al. Glucocorticoids modulate TGF-β production by human fetal lung fibroblasts. Inflammation 2003; 27: 9–19.
33. Wu J, Rnjak-Kovacina J, Du, Y, Funderburgh ML, Kaplan DL, Funderburgh JL. Corneal stromal bioequivalents secreted on patterned silk substrates. Biomaterials 2014; 35: 3744–55.
34. Herrmann J, Gressner AM, Weiskirchen R. Immortal hepatic stellate cell lines: useful tools to study hepatic stellate cell biology and function? Journal of Cellular and Molecular Medicine 2007; 11: 704–22.

Received: 05/10/2016
Accepted: 15/11/2016

ORIGINAL ARTICLE

Transseptal Suturing Reduce Patient Anxiety after Septoplasty Compared to Nasal Packing

Kamran Sari[1,], Ali Irfan Gul[2], Yunus Kantekin[1], Ozgul Karaaslan[2], Zeliha Kapusuz Gencer[1]*

[1] Bozok University School of Medicine, Ear Nose & Throat Department, Yozgat, Turkey
[2] Bozok University School of Medicine, Psychiatry Department, Yozgat/Turkey
* Corresponding author: Bozok University School of Medicine, Adnan Menderes Street Number 190, Yozgat/Turkey; e-mail: kamransari@gmail.com

Summary: Background: We measured postoperative anxiety in patients who underwent transseptal suturing or nasal packing after septoplasty. Materials and Methods: Transseptal suturing was performed on Group 1 patients and nasal splints with airway were placed after septoplasty in Group 2 patients. Postoperative 48-h anxiety levels of both groups were measured using the State-Trait Anxiety Inventory (STAI) clinical assessment scale, prior to removal of nasal packing in Group 2. Results: Transseptal suturing was performed after septoplasty in 28 patients and nasal packing in 34 patients. The State-Trait Anxiety Inventory clinical assessment state (STAI-S) and trait (STAI-T) instruments were used to measure postoperative anxiety. The STAI-S scores were found 35.00 in the transseptal suturing group and 43.8 in the nasal packing group; the difference was found significant ($p < 0.05$). The STAI-T scores were found 42.6 in the transseptal suturing group and 45.7 in the nasal packing group; the difference was not found significant ($p > 0.05$). The rate of minor hemorrhage was found 10.7% in Group 1 patients. Conclusions: Transseptal suturing is simple and reliable when performed after septoplasty. The technique is painless and comfortable, and reduces patient anxiety (compared to that associated with nasal packing) with only a minor increase in operating time and hemorrhage.

Keywords: *Septoplasty; Nasal packing; Transseptal suturing;Aanxiety*

Introduction

Nasal septum deviation is one of the most common disorders treated in Ear Nose & Throat (ENT) clinics. Septoplasty is very common. Nasal packing is often applied after surgery, primarily to control bleeding, but also to stabilize the cartilaginous and bony skeleton of the nose (1). Nasal packs prevent septal hematoma after surgery. However, removal of nasal packs may be painful. Also, some complications are associated with nasal packing; these include mucosal injury, septal perforation, and eustachian tube dysfunction (1, 2). Rarely, sleep respiratory disturbances, reduced arterial oxygen saturation during sleep, and toxic shock syndrome, may develop (3, 4). Therefore, transseptal suturing has been developed as an alternative. An important advantage of such suturing is that the pain caused by nasal packing is eliminated. Also, respiration is not affected and suture removal is easy, reducing patient anxiety (5).

Anxiety disorders are very common psychiatric conditions, with a lifetime prevalence of about 17% (6) Both physical problems and environmental factors can induce anxiety. Surgery may increase anxiety levels either preoperatively or postoperatively.

We investigated postoperative anxiety levels in patients undergoing transseptal suturing or nasal packing after septoplasty.

Materials and Methods

This was a prospective cross-sectional study on 62 patients with nasal septum deviations. All patients were referred to our Department of Otorhinolaryngology, Head and Neck Surgery, between May 2014 and October 2015. Written informed consent was obtained from each patient and our local Ethics Committee approved the work. The study was performed in accordance with the ethical principles of the Declaration of Helsinki. Detailed ENT and physical examinations were performed on all patients. The exclusion criteria included concha bullosa, nasal polyps, and any additional nasal or paranasal pathology. Septoplasty was performed on all patients under general anesthesia. In septoplasty surgery hemitransfixion incision was performed. Deviated bone and cartilage parts were removed. L strut was left. All operations were performed by the same surgeon. Patients were randomly divided into two groups. Transseptal suturing was performed on Group 1 patients and nasal splints with airway were placed after septoplasty in Group 2 patients. During the transseptal suture method, the nasal septum was sutured using a 3/0 vicryl suture (Vicryl 3/0 absorbable suture, Sinorgmed®, Shandong, China). We placed four separate horizontal transseptal mattress sutures (Figure 1) (7, 8). All patients were followed-up after surgery. Postoperative 48-h anxiety levels of both groups were

https://doi.org/10.14712/18059694.2017.40
© 2016 Charles University. This is an open-access article distributed under the terms of the Creative Commons Attribution License (http://creativecommons.org/licenses/by/4.0), which permits unrestricted use, distribution, and reproduction in any medium, provided the original author and source are credited.

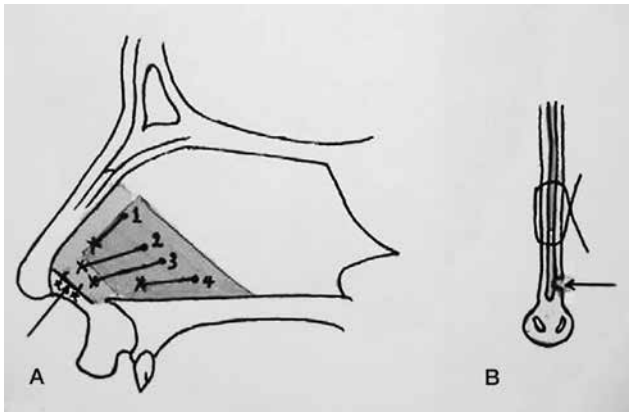

Fig. 1: Septal suturing technique. (A) Lateral view of the nose. The first suture is is inserted just below the dorsal part of the L-strut segment. This will act as a support especially when cartilage is removed from the dorsal part of the L-strut segment. (B) Axial view of the nose. It is demonstrated a separate through and through horizontal mattress suture passing through both sides of the septal mucuperichondrial flaps. Arrow, incision line; red area, removed area; yellow area, L-strut. (With the permission from Dr. Ardehali.)

measured using the State-Trait Anxiety Inventory (STAI) clinical assessment scale, prior to removal of nasal packing in Group 2.

STAI (State-Trait Anxiety Inventory clinical assessment scale)

The STAI was developed by Spielberger et al. (9) and measures state and trait anxiety in subjects > 14 years of age of normal mental development. The STAI contains two forms: the STAI State (STAI-S) and STAI Trait (STAI-T).

The STAI-S measures the anxiety level at a specific time under certain conditions. In the state measure the participant was asked to answer "What degree do you feel at this moment?" Emotional state of each item has four response alternatives. These are "Not at all," "Somewhat," "Moderately so," and "Very much so". The STAI-T measures the anxiety level independent of the current conditions. In the trait measure, the participant was asked to answer "How often do you generally feel?" Each item has four response alternatives. "Almost never," "Sometimes," "Often," and "Almost always". Responses were scored by the Likert scoring method (i.e., 1–2-3–4). A higher score indicated a higher anxiety level (10). The STAI is simple, and is self-completed. Both forms can be completed at the same sitting. First, the STAI-S form is completed, followed by the STAI-T. The Turkish version of the STAI questionnaire that we used has been validated in a Turkish population (11). Both the STAI-S and STAI-T responses are graded as follows: 1 (*rarely*); 2 (*sometimes*); 3 (*a lot of the time*); and 4 (*almost always*). The scores range from 20 to 80, and higher scores indicate more anxiety (12).

Statistical analysis

Anxiety levels were compared using SPSS for Windows software (ver. 18.0; SPSS Inc., Chicago, IL, USA). Descriptive data are presented as means and standard deviation (SD) for normally distributed variables. The normality of each variable was tested using the one-sample Kolmogorov-Smirnov test. No variable had a normal distribution. The chi-squared test was used to compare categorical variables between the groups. The Mann-Whitney U-test was used to evaluate between-group differences in continuous variables. A p-value <0.05 was considered to reflect statistical significance.

Results

The transseptal suturing group contained 28 patients (21 male, 7 female; mean age = 32.03 ± 12.3 years) and the nasal packing group contained 34 patients (25 male, 9 female; mean age = 30.02 ± 11.9 years). Patient age did not differ significantly between the groups (p = 0.474). The STAI-S scores were 35.00 ± 6.99 in the transseptal suturing group and 43.8 ± 13.9 in the nasal packing group; the difference was significant (p = 0.014). The STAI-T scores were 42.6 ± 7.6 in the transseptal suturing group and 45.7 ± 11.7 in the nasal packing group; the difference was not significant (p = 0.335) (Table 1). The anxiety level did not differ by gender in either group (Table 2).

Tab. 1: The STAI-S-1 and STAI-S-2 scores of both groups.

	Gender	Age	STAI-S Mean ± SD	STAI-T	Surgical time
Group1 (n = 28)	Male 21, Female 7	Mean 33.3	35.0 ± 6.99	42.6 ± 7.6	48.4 ± 6.02 min
Group 2 (n = 34)	Male 25, Female 9	Mean 30.01	43.8 ± 13.9	45.7 ± 11.7	41.8 ± 5.9 min
p value		0.474	0.024	0.335	<0.001
Z value		−0.717*	−2.252*	−0.964*	−4.155*

min = minute, SD (Standard Deviation)
*Mann-Whitney U Test

Tab. 2: STAI-S and STAI-T scores by gender.

			STAI-S	STAI-T
Male	Transseptal suture group	n = 21	35.7 ± 10.6	40.5 ± 5.5
	Nasal Pack group	n = 25	41.8 ± 14.2	44.9 ± 12.3
p value			0.145	0.400
Z value*			−1.458	−0.842
Female	Transseptal suture group	n = 7	37.0 ± 8.6	48.5 ± 10.2
	Nasal Pack group	n = 9	49.3 ± 12.4	48.0 ± 10.8
p value			0.060	0.832
Z value*			−1.882	−0.213

*Mann-Whitney U Test.

The mean surgical times were 48.4 ± 6.02 and 41.8 ± 5.9 min in patients of Groups 1 and 2, respectively; the difference was significant ($p < 0.001$).

One postoperative infection developed at the incision site of a Group 1 patient. Minor hemorrhage was observed in three Group 1 patients and was stopped successfully. No major hemorrhage, septal hematoma, perforation, or abscess was observed in either group postoperatively.

Discussion

Septoplasty is one of the most common nasal surgeries performed in otolaryngology clinics. Traditionally, nasal packing has been applied after septoplasty to control postoperative bleeding and stabilize the nasal septum. Many forms of nasal packing are available, including Merocel, "rapid rhino", the "Doyle pack", gauze with vaseline, and synthetic polyurethane. These are placed after surgery to prevent bleeding, septal hematoma, and septal abscess (13, 14). Although the packs afford many advantages, they increase the risk of infection and cause pain (15). Complications include eustachian tube dysfunction, middle ear effusion, and obstruction of the larynx. Also, 50–68% of the cilia of the surface mucosa may be functionally compromised by packing, and sinus infections can develop (16, 17). Packs can also cause mouth dryness and a sore throat. Aspiration and cardiological complications can also occur (1).

Removal of nasal packs causes serious pain, and can trigger significant patient anxiety. In recent years, transseptal suturing has been developed as an alternative to packing (18). Such suturing reduces patient pain and anxiety caused by respiratory problems and/or pack removal. Therefore, we compared the postoperative anxiety levels of patients with nasal packs (before pack removal) and those who underwent transseptal suturing. The STAI-S scores were lower in the transseptal suturing group than the nasal packing group ($p < 0.05$). However, the STAI-T scores were similar in the two groups. We suggest that this is because the STAI-T test evaluates general attitudes and feelings. We found that patients were anxious before removal of nasal packing. In addition not only decreased nasal breathing but also fear of packing removal can influence anxiety status in patients. Transseptal suturing may decrease postoperative pain and anxiety, improving the quality of life. Hosemann et al. (19) measured perioperative pain and anxiety levels in patients undergoing endoscopic sinus surgery, and compared three different types of nasal packing. Female gender, and detailed preoperative information on the surgical procedure, were associated with much more postoperative anxiety. For anxious patients, it was recommended that nasal packing should at least partially preserve nasal breathing. We found no significant association between gender and anxiety levels. Muluk et al. (20) tested the validity of Hospital Anxiety and Depression Scale (HADS) data from patients who underwent nasal surgery. They enrolled 50 adult patients who underwent nasal surgery for various reasons. Bilateral nasal packing was applied to all patients for 2 days. The anxiety and depression levels did not change significantly postoperatively. Thus, if patients were well-informed about nasal packing and hospital procedures prior to surgery, nasal packing was not associated with psychological trauma. It was observed that the HADS aided the diagnosis of emotional disorders, especially in patients who were hospitalized long-term. Rozanska-Kudelska et al. (21) studied the depression and anxiety symptoms of patients undergoing endoscopic sinus surgery, both before and after surgery. The levels of anxiety and depression were assessed using the Beck Depression Inventory (BDI) and the HADS. The BDI and HADS scores decreased significantly after surgery. It was claimed that high-quality treatment and improvement in somatic status enhanced the mental state and quality of life.

In all cited studies, anxiety and depression were measured both preoperatively and postoperatively. We did not apply the STAI preoperatively, because our aim was to measure the anxiety levels of patients just before removal of nasal packs and to compare these levels to those of patients without nasal packs.

The mean surgical time was somewhat longer in the transseptal suturing than the nasal packing group; the literature indicates that the mean surgical time was much longer previously (7, 8, 22). A postoperative infection developed at the incision site of only one Group 1 patient, and responded to antibiotics. No postoperative septal hematoma, septal perforation, or major bleeding was observed in any patient.

The rate of minor hemorrhage has been reported as 2.3% in transseptal suturing septoplasty (23). In our study the rate was 10.7%. Especially in the postoperative 24 hours minor hemorrhages are encountered frequent. These hemorrhages can be controlled with minor interventions, and usually no nasal packing is required. In our study no major hemorrhage, septal hematoma and septal perforation was encountered in any patient.

Conclusion

Transseptal suturing is simple and reliable and can be safely performed after septoplasty. Although the operating time may increase slightly, the technique is painless and comfortable and reduces postoperative anxiety caused by nasal packing.

References

1. Ardehali MM, Bastaninejad S. Use of nasal packs and intranasal septal splints following septoplasty. Int J Oral Maxillofac Surg 2009; 38: 1022–24.
2. Thompson AC, Crowther JA. Effect of nasal packing on eustachian tube function. The J Laryngol Otol 1991; 105: 539–40.
3. Wagner R, Toback JM. Toxic shock syndrome following septoplasty using plastic septal splints. Laryngoscope 1986; 96: 609–10.
4. Yigit O, Cinar U, Uslu B, Akgul G, Topuz E, Dadas B. The effect of nasal packing with or without an airway on arterial blood gases during sleep. Kulak Burun Bogaz Ihtis Derg 2002; 9: 347–50.
5. Turhan M, Bostanci A, Akdag M, Dinc O. A comparison of the effects of packing or transseptal suture on polysomnographic parameters in septoplasty. Eur Arch Otorhinolaryngol 2013; 270: 1339–44.
6. Somers JM, Goldner EM, Waraich P, Hsu L. Prevalence and incidence studies of anxiety disorders: a systematic review of the literature. Can J Psychiatry 2006; 51: 100–13.
7. Korkut AY, Teker AM, Eren SB, Gedikli O, Askiner O. A randomised prospective trial of trans-septal suturing using a novel device versus nasal packing for septoplasty. Rhinology 2010; 48: 179–82.
8. Lemmens W, Lemkens P. Septal suturing following nasal septoplasty, a valid alternative for nasal packing? Acta Otorhinolaryngol Belg 2001; 55: 215–21.
9. Spielberger CD GR, Lushene RE. Manuel for State-Trait Anxiety Inventory (Self-Evaluation Questionnaire). 2nd ed. California: Consulting Psychologists Press,1970: 20–21.
10. Iwata N, Mishima N, Shimizu T, et al. The Japanese adaptation of the STAI Form Y in Japanese working adults – the presence or absence of anxiety. Ind Health1998; 36: 8–13.
11. AK Ö. Sürekli öfke (SL-Öfke) ve öfke ifade tarzı (Öfke tarz) ölçekleri ön çalışması. (Pre-evaluation of state and trait anxiety inventories). Türk Psikoloji Dergisi 1994; 9: 26–35.
12. Song QH, Xu RM, Zhang QH, Ma M, Zhao XP. Relaxation training during chemotherapy for breast cancer improves mental health and lessens adverse events. Int J Clin Exp Med 2013; 25: 979–84.
13. Hesham A, Ghali A. Rapid Rhino versus Merocel nasal packs in septal surgery. J Laryngol Otol 2011; 125: 1244–46.
14. Kim YS, Kim YH, Kim NH, Kim SH, Kim KR, Kim KS. A prospective, randomized, single-blinded controlled trial on biodegradable synthetic polyurethane foam as a packing material after septoplasty. Am J Rhinol Allergy 2011; 25: 77–9.
15. Banglawala SM, Gill M, Sommer DD, Psaltis A, Schlosser R, Gupta M. Is nasal packing necessary after septoplasty? A meta-analysis. Int Forum Allergy Rhinol 2013; 3: 418–24.
16. Abram AC, Bellian KT, Giles WJ, Gross CW. Toxic shock syndrome after functional endonasal sinus surgery: an all or none phenomenon? Laryngoscope 1994; 104: 927–31.
17. Shaw CL, Dymock RB, Cowin A, Wormald PJ. Effect of packing on nasal mucosa of sheep. J Laryngol Otol 2000; 114: 506–09.
18. Certal V, Silva H, Santos T, Correia A, Carvalho C. Trans-septal suturing technique in septoplasty: a systematic review and meta-analysis. Rhinology 2012; 50: 236–45.
19. Hosemann W, Loew TH, Forster M, Kuhnel T, Beule AG. Perioperative pain and anxiety in endoscopic sinus surgery. Laryngorhinootologie 2011; 90: 476–80.
20. Muluk NB, Oguzturk O, Ekici A, Koc C. Emotional effects of nasal packing measured by the Hospital Anxiety and Depression Scale in patients following nasal surgery. J Otolaryngol 2005; 34: 172–77.
21. Rozanska-Kudelska M, Szulc A, Matulka M, Simonienko K, Rogowski M. Quality of life, depression and anxiety symptoms in patients with chronic rhinosinusitis with polyps treated by endoscopic sinus surgery. Pol Merkur Lekarski 2012; 32: 228–31.
22. Ozkiris M, Kapusuz Z, Saydam L. Comparison of nasal packs with transseptal suturing after nasal septal surgery. Am J Otolaryngol 2013; 34: 308–11.
23. Siegel NS, Gliklich RE, Taghizadeh F, Chang Y. Outcomes of septoplasty. Otolaryngol Head Neck Surg 2000; 122: 228–32.

Received: 19/07/2016
Accepted: 08/12/2016

CASE REPORT

Intraparenchymal Epididymal Cyst (IEC) 4 cm in Diameter in a 15-Year Old Male Patient; a Case Report and Review of the Literature

Dimitrios Patoulias*, Maria Kalogirou, Ioannis Patoulias

1st Department of Pediatric Surgery, Aristotle University of Thessaloniki, GH G. Gennimatas, Thessaloniki, Greece
* Corresponding author: M. Alexandrou 3B, Peuka, Thessaloniki, Postal code 57010; e-mail: dipatoulias@gmail.com

Summary: Intraparenchymal epididymal cysts (IECs) are benign cystic formations of the epididymis of unknown pathogenesis, which typically appear in adolescence or adulthood. In patients older than 14 years old their prevalence is doubled. After systematic and thorough research of the current literature, we did not find another case report of intraparenchymal epididymal cyst with similar dimensions. The male patient, 15 years old, visited our outpatient department complaining of pain in the right hemiscrotum. Diagnosis of IEC was confirmed after the conduction of ultrasound examination. Patient underwent surgical exploration of the right hemiscrotum. Resection of the IEC followed. Postoperative course was uneventful, with recession of the symptoms. In our opinion, IECs should be surgically removed, either when they are symptomatic or when they are asymptomatic, but of a diameter greater than 1 cm and without regression tendency.

Keywords: *Intraparenchymal epididymal cyst (IEC); Epididymis; Painful hemiscrotum*

Introduction

Intraparenchymal epididymal cysts (IECs) are benign, single spaced, containing serous fluid, formations, lined by cuboidal or columnar epithelium (1, 2). Accidental identification of an IEC occurs in 0.8% of all adolescents that undergo ultrasound examination of the scrotum (1). Nidzielski J. et al. (1) studied 45 cases of adolescents with IECs, noting that in 75–80% they were solitary, in 20% there were 2 cysts and in 5% there were 3 or more cysts, unilateral or bilateral. It is in fact an extratesticular cystic lesion, similar to spermatocele, regarding to the composition of the fluid and the histological structure of its capsule. They differ in: a) the localization, because spermatocele originates from the head of the epididymis, while IEC can originate from every region of the epididymis and b) the composition of the containing fluid. In spermatocele it consists of sperm cells, lymphocytes and cellular debris. Fluid cannot be serous, but milky as well (3).

Aim of this study is to present a case of an adolescent with an IEC 4 cm in diameter – especially after noticing that there are no case reports of IECs of such a diameter in current literature – and our proposal on the appropriate diagnostic and therapeutic approach.

Case report

A 15 years old male patient with free medical history visited our outpatient department complaining of the presence of a lump that he first palpated in the right hemiscrotum 12 months ago during self-examination. He reported mild pain, exacerbating in the context of physical activity. During inspection of the scrotum there were no signs of inflammation, but the cyst protruded as an intrascrotal mass above the right testicle. Further physical examination revealed the presence of a sizeable, painless, fluctuating lesion in the upper right hemiscrotum, clearly distinguished from the ipsilateral testis. Transillumination was indicative of a rather cystic lesion. Right testicle was orthotopic, painless when palpated, while it was impossible to distinguish the boundaries between the epididymis and the lesion. No other

Fig. 1: IEC 4 cm in diameter, which occupies the head and the body of the epididymis.

https://doi.org/10.14712/18059694.2017.41
© 2016 Charles University. This is an open-access article distributed under the terms of the Creative Commons Attribution License (http://creativecommons.org/licenses/by/4.0), which permits unrestricted use, distribution, and reproduction in any medium, provided the original author and source are credited.

pathological manifestations were detected at the rest of the scrotum and groin.

A single spaced, thin walled, cystic lesion, within the parenchyma of the head and the body of the right epididymis, 4 cm in diameter was depicted in the ultrasound. The two testes had normal imaging features, with dimensions 26 × 17 × 14.5 mm the right and 25.8 × 17.2 × 13.8 mm the left. Imaging evaluation of the rest scrotal structures, the groin and the urinary tract was normal.

Elective surgical procedure under endotracheal anesthesia followed. Access was achieved by a transverse incision in the middle of the right hemiscrotum, followed by the transection of the dartos, the external spermatic fascia, the cremasteric fascia, the internal spermatic fascia, the parietal and visceral tunica vaginalis and the externalization of the testis and the epididymis. IEC on the head and the body of the epididymis was identified. Careful enucleation of the cyst followed (Figure 1).

Epididymal capsule was sutured continuously by using Vigryl rapid 6/0. Testis and epididymis were repositioned in the ipsilateral hemiscrotum, followed by the closure of the surgical wound in the anatomical order.

Results

Postoperative period was uncomplicated and the patient was discharged home on the first postoperative day. Histopathological report described a cystic lesion with smooth transparent wall and a transitional epithelial lining, containing serous fluid, but no spermatozoa. Three years later, after a thorough follow-up on a 6-month basis, patient is free of any complication or relapse or accompanying correlating signs.

Discussion

IEC is often identified in patients with cryptorchidism, cystic fibrosis, Von Hippel-Lindau disease, polycystic kidney disease, as well after prenatal exposure to diethylstilbestrol (2, 4, 5). The incidence of IECs doubles after the age of 14 years (1, 6). Sempere CFS et al. (7) studied cases of 15 boys with IECs aged 1–16 years old (average 11.5 years). Left varicocele co-existed with IEC in 40% of these patients (6/15), while 26% of the patients (4/15) had a medical history of orcheoepididymitis. Finally, in half of these cases, diagnosis of an IEC was made accidentally, while the patient underwent physical examination for another reason. Thus, they emphasize on the need of thorough diagnostic approach in patients with IEC, in order to confirm or exclude the presence of varicocele.

Differential diagnosis should include intrascrotal cystic lesions, which are divided – based on their localization- into intratesticular (testicular cyst, tunica albuginea cyst, epidermoid cyst) and extratesticular (epididymal cystic lymphangioma, spermatocele, paratesticular abscess, epididymal adenomatoid tumor, varicocele) (3). Absence of spermatozoa in the cyst's fluid and its attachment to the head and the body of the epididymis contributed to the exclusion of spermatocele in our case (8).

Regarding to the pathogenesis of IECs the following cited might play a significant role: a) hormonal disorders stemming from toxic agents acting either prenatally (such as diethylstilbestrol or Cannabis indica) or after birth (9, 10, 11), b) the degenerative process and c) the existence of obliteration or stenosis of the epididymal ducts with subsequent pro-stenotic dilatation. The latter evolves progressively, leading to the development of a cystic lesion, which possibly exerts pressure on the adjacent seminiferous tubules (3). This etiologic approach is strengthened by the observation of Blau et al. (12) on the incidence of IECs in patients with cystic fibrosis. Cystic fibrosis is associated with the absence of the vas deferens in 90% of all cases. Based on this etiologic approach, the peripheral obstruction of the secretory system leads to the cystic dilatation of the epididymal secretory system and finally the development of an IEC.

Sharpe RM et al. (13) and Skakkebaek NE et al. (14) consider as possible the correlation between the IECs and the testicular dysgenesis syndrome. Wollin M. et al. (15) believe that the IEC results from the progressive dilatation of the vestigial remnants, which do not communicate with the secretory epididymal ducts. If it is considered as a result of cystic dysplasia of the affected epididymis, with the impaired development of the mesonephric duct being the embryological substrate, then preventive ultrasound examination of the kidneys is absolutely indicated. In our case, we conducted also an ultrasound scan of the kidneys during the preoperative period (16). Belet U. et al. (17) emphasize on the necessity of the exclusion of autosomal inherited polycystic kidney disease, which can co-exist with IEC.

In our case, IEC was 4 cm in diameter, finding that suggests that lesion's dimensions may be greater than those reported so far in the literature. In our case, it is possible that the size of IEC gradually increased, however, due to the patient's age, parents could not have noticed the scrotal mass. Erikci V. et al. (18) reported 42 patients with IEC (22 left, 16 right and 4 bilateral), aged from 2 months to 16 years old (average 10.7 years). Cysts' diameter ranged from 2 to 20 mm. Hegazy AF. et al. (11) studied 20 boys aged from 3 months to 15 years old (average 11.5 years) with IEC from 0.3 to 3 cm in diameter. Pieri S. et al. (19) treated 25 patients with symptomatic IEC, 5 cm or greater in diameter. However, all the patients that underwent treatment were adults.

Ameli M. et al. (20) reported a case of a torsion of an epididymal cyst (4 × 4 × 3 cm) in a 14-year old boy. However, it was a case of appendiceal torsion (embryonic remnant of epididymis) and not a case of an IEC.

Homayoon K. et al. (2) studied 20 patients with identified IEC. Patient's average age at diagnosis was 10.5 years. 15 patients presented complaining of a palpable scrotal mass, while 4 patients suffered from scrotal pain. Cysts' diameter ranged from 3 to 30 mm.

The context of treatment of an IEC is determined by the cyst's diameter, the symptomatology and the development of

complications (3, 6, 21). 51.8–75% of the cysts are asymptomatic, found accidentally during physical examination, while 25–49.2% of them are symptomatic (2, 6) and 50% of them regresses automatically within the next 3–35 months (average 18 months) (2). Conservative approach should be selected in patients with asymptomatic IEC, less than 1 cm in diameter. On the other hand, elective surgical removal should be conducted when: a) the IEC is asymptomatic, greater than 1 cm, without regression tendency after 12 month surveillance (18), b) the IEC is symptomatic, regardless of its diameter and c) there are signs and symptomatology of acute scrotum due to inflammation, intracystic bleeding or secondary epididymal torsion. In our case, surgical treatment was absolutely indicated, due to the presence of persistent symptoms for at least 4 months and the large diameter of the cyst, greater than all those that are described in patients of the same age in literature. Indicated method of treatment in childhood is the open surgical approach through scrotal incision, either transverse or on the scrotal raphe. Operative strategies in the treatment of IECs and spermatocele in young adults are almost the same. Kauffman EC et al. (22) and Cagiu C. et al. (23) attempted the microscopic assisted spermatocelectomy in order to prevent accidental epididymal injury. It is possible that the microscopic assisted resection of IECs will be the preferable treatment option in the future. Hegazy AF et al. (11) and Pieri S et al. (19) described a conservative technique, consisting of puncture of the IEC, aspiration of its fluid and injection of polidocanol. This technique has been attempted in adults, but not in childhood yet (11).

Despite the thorough approach and resection of the IEC in our case, the possibility of accidental epididymal injury because of immediate vicinity of the efferent epididymal tubules, which could lead to infertility in the future, cannot be excluded. Based on this hypothesis, we believe that a periodic follow-up of the patient and the conduction of spermiogram in a reasonable time are required. Besides, according to the clinical study conducted by Weatherly D. et al. (24), who encountered 91 men, IECs are not related to infertility ($\chi^2_{(df=1)} = 0.362$, $p = 0.55$).

Conflict of interest

None of the contributing authors have any conflict of interest, including specific financial interests or relationships and affiliations relevant to the subject matter or materials discussed in the manuscript.

References

1. Niedzielski J, Miodek M, Krakos M. Epididymal cysts in childhood – conservative or surgical approach? Pol Przegl Chir 2012; 84: 406–10.
2. Homavoon K, Suhre CD, Steinhardt GF. Epididymal cysts in children: natural history. J Urol 2004; 171: 1274–6.
3. Woodward PJ, Scwab CM, Sesterhenn IA. From the archives of the AFIP: extratesticular scrotal masses: radiologic-pathologic correlation. Radiographics 2003; 23(1): 215–40.
4. Steinhardt GF. Editorial comment to epididymal cyst: Not always a benign condition. Int J Urol 2012; 20: 458.
5. ML Leung, GA Gooding and RD Williams. High-resolution sonography of scrotal contents in asymptomatic subjects. American Journal of Roentgenology 1984; 143: 161–164.
6. Posey ZQ, Ahn HJ, Junewick J, Chen JJ, Steinhardt GF. Rate and associations of epididymal cysts on pediatric scrotal ultrasound. J Urol 2010; 184: 1739–42.
7. Chillón Sempere FS, Domínguez Hinarejos C, Serrano Durbá A, et al. Epididymal cysts in childhood. Arch Esp Urol 2005; 58(4): 325–8.
8. Munden MM, Trautwein LM. Scrotal pathology in pediatrics with sonographic imaging. Curr Probl Diagn Radiol 2000; 29(6): 185–205.
9. Baskin LS, Himes K, Colborn T. Hypospadias and endocrine disruption: is there a connection?. Environ Health Perspect 2001; 109(11): 1175–83.
10. Paulozzi LJ. International trends in rates of hypospadias and cryptorchidism, Environ Health Perspect 1999; 107(4): 297–302.
11. Hegazy AF, Atrebi M. Management challenges of epididymal cysts in childhood. Med J Cairo Univ 2012; 80: 909–12.
12. Blau H, Freud E, Mussaffi H, et al. Urogenital abnormalities in male children with cystic fibrosis. Arch Dis Child 2002; 87(2): 135–8.
13. Sharpe RM: hormones and testis development and possible adverse effects of environmental chemicals. Toxicol Lett 2001; 120: 221.
14. Skakkebaek NE, Rajpert-Demeyts E. testicular dysgenesis syndrome: an increasingly common developmental disorder with environmental aspects. Hum Reprod 2001; 16: 972.
15. Wollin M, Marshall FF, Fink MP, et al. Aberrant epididymal tissue: a significant clinical entity. J Urol 1987; 138(5): 1247–50.
16. Nistal M, González-Peramato P, Sousa G, et al. Cystic dysplasia of the epididymis: a disorder of mesonephric differentiation associated with renal maldevelopment. Virchows Arch 2010; 456(6): 695–702.
17. Belet U, Danaci M, Sarikaya S, et al. Prevalence of epididymal, seminal vesicle, prostate, and testicular cysts in autosomal dominant polycystic kidney disease. Urology 2002; 60(1): 138–41.
18. Erikci V, Hoşgör M, Aksoy N, et al. Management of epididymal cysts in childhood. J Pediatr Surg 2013; 48(10): 2153–6.
19. Pieri S, Agresti P, Morucci M, et al. A therapeutic alternative in the treatment of epididymal cysts: percutaneous sclerotherapy. Radiol Med 2003; 105(5–6): 462–70.
20. Ameli M, Boroumand-Noughabi S, Gholami-Mahtaj L. A 14-Year-Old Boy with Torsion of the Epididymal Cyst. Case Reports in Urology 2015, Article ID 731987, 3 pages.
21. Steinhardt GF. Editorial comment to epididymal cyst: Not always a benign condition. Int J Urol 2012; 20: 458.
22. Kauffman EC, Kim HH, Tanrikut C, et al. Microsurgical spermatocelectomy: technique and outcomes of a novel surgical approach, J Urol 2011; 185(1): 238–42.
23. C. Gagiu, S. Voinea, I. Manea, et al. Microscopic assisted spermatocelectomy – a fertility preserving procedure. Revista Română de Urologie 2015; 14(2); 63–5.
24. Weatherly D, Wise PG, Mendoca S, et al. Epididymal Cysts: Are They Associated With Infertility?. Am J Mens Health. 2016 Apr 26. pii: 1557988316644976. [Epub ahead of print]

Received: 13/09/2016
Accepted: 02/12/2016

CASE REPORT

A Case of 2-Year-Old Child with Entero-Enteric Fistula Following Ingestion of 25 Magnets

Zenon Pogorelić[1], Matija Borić[2], Joško Markić[3], Miro Jukić[1], Leo Grandić[2]*

[1] Department of Pediatric Surgery, Split University Hospital and University of Split, School of Medicine, Split, Croatia
[2] Department of Surgery, Split University Hospital and University of Split, School of Medicine, Split, Croatia
[3] Department of Pediatrics, Split University Hospital and University of Split, School of Medicine, Split, Croatia
* Corresponding author: Department of Pediatric Surgery, Split University Hospital, Spinčićeva 1, 21 000 Split, Croatia; e-mail: zpogorelic@gmail.com

Summary: Introduction: Magnet ingestion usually does not cause serious complications, but in case of multiple magnet ingestion or ingestion of magnet with other metal it could cause intestinal obstruction, fistula formation or even perforation. Case report: We report case of intestinal obstruction and fistula formation following ingestion of 25 magnets in a 2-year-old girl. Intraoperatively omega shaped intestinal loop with fistula caused by two magnetic balls was found. Intestine trapped with magnetic balls was edematous and inflamed. Resection of intestinal segment was performed, followed by entero-enteric anastomosis. A total of 25 magnets were removed from resected intestine. Conclusion: Single magnet ingestion is treated as non-magnetic foreign body. Multiple magnet ingestion should be closely monitored and surgical approach could be the best option to prevent or to cure its complications.

Keywords: *Ingestion; Magnetic foreign body; Multiple magnets; Intestinal fistula; Children*

Introduction

Ingested foreign bodies are a common problem throughout the world. More than three quarters of foreign body ingestions occur in children (1). In 90% of cases swallowed foreign bodies pass harmlessly through the gastrointestinal tract. However, around 10–20% of foreign body ingestions require endoscopic removal, and around 1% will require surgical intervention (2). Some of foreign bodies require special considerations, such as batteries and magnets (3, 4). In the last decade the incidence of ingested magnets has grown due to increased use of magnetic toys (4). Single magnet ingestion usually ends spontaneously and do not cause serious complications that require surgical intervention but in case of multiple magnet ingestion or ingestion of magnet with other metal it could cause intestinal obstruction, fistula formation or even perforation (5, 6).

Here we present a case of intestinal obstruction and fistula formation following ingestion of 25 magnets in a 2-year-old girl.

Case report

A previously healthy 2-year-old girl presented to our surgical emergency department, because of ingestion of several small, spherical magnets earlier that morning. Parents did not see her swallowing those magnets, but they suspected it, and estimated number of around 20–25 magnets. Physical examination was unremarkable; abdomen was soft and flat, with no signs of peritoneal irritation. Initial abdominal X-ray revealed a metallic foreign body V-shaped necklace formation in middle abdomen (Fig. 1). Based on unchanged clinical status, with no fever, no lethargy or abdominal pain, with all vital signs being normal, the patient was discharged from hospital. The parents got instructions to monitor her stool, and got instructions and description of signs of possible complications. The patient was on repeated follow-ups where unchanged vital signs were found. Repeated abdominal X-ray revealed aboral progression of magnets, but still not reaching the colon (Fig. 2). Nine days following foreign body ingestion, the child was brought back to hospital because she had refused any food. Examination showed that the patient appeared dehydrated with distended, but soft abdomen, with no signs of peritoneal irritation. Following X-ray and laboratory test, along with discussion of potential risks and benefits of surgical treatment, exploratory laparotomy through lower midline incision was performed. Around 100 cm aboral to the ligament of Treitz omega shaped intestinal loop with fistula caused by two magnetic balls was found (Fig. 3). Intestine trapped into magnetic balls was edematous and inflamed. Resection of intestinal segment was performed, followed by entero-enteric anastomosis. A total of 25 magnets were removed from resected intestine (Fig. 4). After the surgery the child was admitted to De-

ACTA MEDICA (Hradec Králové) 2016; 59(4):140–142
https://doi.org/10.14712/18059694.2017.42

© 2016 Charles University. This is an open-access article distributed under the terms of the Creative Commons Attribution License (http://creativecommons.org/licenses/by/4.0), which permits unrestricted use, distribution, and reproduction in any medium, provided the original author and source are credited.

Fig. 1: Initial abdominal X-ray – a metallic foreign body: V-shaped necklace formation in middle abdomen.

Fig. 2: Abdominal X-ray on 5th day after ingestion of foreign body – aboral progression of magnets.

partment of pediatric surgery. The patient recovered well postoperatively and she was discharged home on the 5th postoperative day. At regular follow ups no complications were recorded.

Discussion

Ingestion of foreign bodies is a common pediatric problem, with more than 100 000 cases annually. The most common ingested foreign bodies are coins, toys, batteries, bones or food. Magnets are increasingly ingested (7). Magnets have evolved rapidly in the past three decades. Neodymium magnets were created in 1980s and have much stronger adherence than previously used magnets (8). US National Electronic Injury Surveillance System described 8.5 times increase of possible ingestion of magnets in underage children in last decade (9). Thus Canadian and USA healthcare institutions have intention to regulate laws to keep strong magnets out of the hands of children (10).

Single magnet ingestion is like swallowing any non-magnetic foreign body, while multiple magnets can cause serious gastrointestinal complications like entero-enteric fistula formation, bowel with associated perforation, peritonitis, and bowel ischemia or necrosis (11, 12).

In our case magnets were beyond ligament of Treitz and proximal to the terminal ileum. Management of asymptomatic patients in that descripted position is more controversial than in other gastrointestinal part where foreign body could

Fig. 3: Intraoperative findings – omega shaped intestinal loop with fistula caused by magnetic balls.

be reached either by esophagogastroduodenoscopy or colonoscopy. Laparotomy and laparoscopy interventions required in case of intermediate position of magnets in gastrointestinal tract increase morbidity and mortality (13). Therefore, conservative therapy should be observed as possible therapeutic option. The consensus of North American Society for Pediatric Gastroenterology, Hepatology, and Nutrition experts suggest conservative approach only in case of direct patient observation (11). Prevention is crucial for this rapidly increasing problem (1). Awareness of possible magnet ingestion as well as potential complications of it, leads to reduced time from ingestion to diagnosis and from diagnosis to final solution.

Conclusion

It is important to differentiate single from multiple magnet ingestion. Single magnet ingestion is treated as non-magnetic foreign body. Multiple magnet ingestion should be closely monitored and surgical approach could be the best option to prevent or to cure its complications.

Fig. 4: Resected speciemen – intestinal segment with fistula and 25 removed magnets.

References

1. George AT, Motiwale S. Magnets, children and the bowel: a dangerous attraction? World J Gastroenterol 2012; 18: 5324–5328.
2. Eisen GM, Baron TH, Dominitz JA, et al. Guideline for the management of ingested foreign bodies. Gastrointest Endosc 2002; 55: 802–806.
3. Hussain SZ, Bousvaros A, Gilger M, et al. Management of ingested magnets in children. J Pediatr Gastroenterol Nutr 2012; 55: 239–242.
4. Tavarez MM, Saladino RA, Gaines BA, et al. Prevalence, clinical features and management of pediatric magnetic foreign body ingestions. J Emerg Med 2013; 44: 261–268.
5. Hernandez Anselmi E, Gutierrez San Roman C, Barrios Fontoba JE, et al. Intestinal perforation caused by magnetic toys. J Pediatr Surg 2007; 42: E13–6.
6. Othman MY, Srihari S. Multiple magnet ingestion: The attractive hazardst. Med J Malaysia 2016; 71:211–212.
7. Kay M, Wyllie R. Pediatric foreign bodies and their management. Curr Gastroenterol Rep 2005; 7: 212–218.
8. Sahin C, Alver D, Gulcin N, et al. A rare cause of intestinal perforation: ingestion of magnet. World J Pediatr 2010; 6: 369–371.
9. Abbas MI, Oliva-Hemker M, Choi J, et al. Magnet ingestions in children presenting to US emergency departments, 2002–2011. J Pediatr Gastroenterol Nutr 2013; 57: 18–22.
10. Rosenfield D, Strickland M, Fecteau A. Magnet ingestion by a 3-year-old boy. CMAJ 2013; 185: 972–974.
11. Kramer RE, Lerner DG, Lin T, et al. Management of ingested foreign bodies in children: a clinical report of the NASPGHAN Endoscopy Committee. J Pediatr Gastroenterol Nutr 2015; 60: 562–574.
12. Naji H, Isacson D, Svensson JF, et al. Bowel injuries caused by ingestion of multiple magnets in children: a growing hazard. Pediatr Surg Int 2012; 28: 367–734.
13. Butterworth J, Feltis B. Toy magnet ingestion in children: revising the algorithm. J Pediatr Surg 2007; 42: e3–5.

Received: 30/11/2016
Accepted: 12/12/2016